Darcy Forchheimer Casson Nanofluid flow over a stretching cylinder with Arrhenius Activation Energy and Gyrotactic Microorganisms

Thesis Submitted By

SALIHA MAHMOOD
(01-248182-005)

Supervised By

Prof. Dr. M. Ramzan

A dissertation submitted to the Department of Computer Science, Bahria University, Islamabad as a partial fulfillment of the requirements for the award of the degree of MS (Mathematics)

(Session 2018 - 2020)

Bahria University
Discovering Knowledge

MS-13

Thesis Completion Certificate

Student's Name: **Saliha Mahmood** Registration No**: 59376**

Program of Study: **MS(Mathematics)** Thesis Title:**" Darcy Forchheimer Casson Nanofluid flow over a stretching cylinder with Arrhenius Activation Energy and Gyrotactic Microorganisms,**

It is to certify that the above student's thesis has been completed to my satisfaction and, to my belief, its standard is appropriate for submission for Evaluation. I have also conducted plagiarism test of this thesis using HEC prescribed software and found similarity index at **09%** that is within the permissible limit set by the HEC for the MS/MPhil degree thesis. I have also found the thesis in a format recognized by the BU for the MS/MPhil thesis.

Principal Supervisor's Signature: _____

Date: 01-10-2020 **Name: Prof. Dr. Muhammad Ramzan**

Dedicated to

My Beloved Parents

And

Respected Supervisor

Whose Prayers, Wishes

And Efforts Are An Inspiration.

Acknowledgments

I am thankful to **ALLAH** Almighty, the most Gracious and the most merciful who bestowed me with His great blessings. I am really blessed as He gave me the ability to learn and to achieve my goal. He gave me a source (His beloved **Prophet (PBUH)**) of light and guidance for my way.

My acknowledgment is to my kind, passionate and diligent supervisor, Prof. Dr. M. Ramzan, who supported me with his great opinions and inspirational thoughts. My intense gratitude is to my honorable teachers. In particular, Dr. Jafar Hasnain and Dr. Rizwan-ul-haq who have always been supportive in all of my course work. I'm blessed to have them in my life.

My intense recognition is to my mother, father and my brother who are always real pillars for my encouragement and showed their everlasting love, care and support throughout my life.

I would like to express my special thanks to my seniors and PhD students who were always remained helpful to me. May Allah shower His blessings upon them more than enough.

Saliha Mahmood

Bahria University Islamabad, Pakistan

September 23, 2020

Bahria University

Discovering Knowledge

MS-14A

Author's Declaration

I, **Saliha Mahmood** hereby state that my MS thesis titled **"Darcy Forchheimer Casson Nanofluid flow over a stretching cylinder with Arrhenius Activation Energy and Gyrotactic Microorganisms"** is my own work and has not been submitted previously by me for taking any degree from this university **Bahria University Islamabad** or anywhere else in the country/world. At any time if my statement is found to be incorrect even after my Graduate the university has the right to withdraw/cancel my MS degree.

Saliha

Name of scholar: **Saliha Mahmood**

Registration no: **59376**

Bahria University

Discovering Knowledge

MS-14B

Plagiarism Undertaking

I solemnly declare that research work presented in the thesis titled **"Darcy Forchheimer Casson Nanofluid flow over a stretching cylinder with Arrhenius Activation Energy and Gyrotactic Microorganisms"** is solely my research work with no significant contribution from any other person. Small contribution / help wherever taken has been duly acknowledged and that complete thesis has been written by me.

I understand the zero tolerance policy of the HEC and Bahria University towards plagiarism. Therefore I as an Author of the above titled thesis declare that no portion of my thesis has been plagiarized and any material used as reference is properly referred / cited.

I undertake that if I am found guilty of any formal plagiarism in the above titled thesis even after award of MS degree, the university reserves the right to withdraw / revoke my MS degree and that HEC and the University has the right to publish my name on the HEC / University website on which names of students are placed who submitted plagiarized thesis.

Saliha

Student / Author's Sign:_____

Name of the Student: **Saliha Mahmood**

Abstract

A mathematical model is investigated to scrutinize the Darcy Forchheimer Casson Nanofluid flow over a stretching cylinder with convective heat and mass conditions. The heat and mass transfer phenomena are visualized in the presence of activation energy and gyrotactic microorganisms. Fluid is electrically conducted in the attendance of applied magnetic field. Appropriate transformations procedure is implemented for the transition of partial differential equations to ordinary one and then computer software-based MATLAB function bvp4c is implemented to handle the envisioned mathematical model. The deliberation of numerous parameters versus the velocity, heat and mass transfer and density of gyrotactic microorganisms are portrayed through graphs. It is witnessed that velocity of the fluid is decreased for increasing values of porosity number and the increasing value of activation energy enhances the concentration. Furthermore the microorganisms profile dwindles for increasing estimates of Peclet number. Local Nusselt number, Local Sherwood number and density number of motile microorganisms are evaluated via tables. An outstanding matching is obtained when the results obtained in the current analysis are compared with an established result in the literature.

Contents

List of Tables

List of Figures

Nomenclature

Symbols

u , w	axial and radial velocity components
B_0	magnetic field strength
T	temperature
T_f	heated fluid temperature
T_∞	ambient fluid temperature
C	concentration
C_f	heated fluid Concentration
C_∞	ambient fluid Concentration
U_0	reference velocity
l	characteristic length
k	thermal conductivity
D_B	brownian diffusion coefficient
D_T	thermophoretic diffusion coefficient
h	convective heat transfer coefficient
k_m	wall mass transfer coefficient
a	radius of cylinder
D_m	molecular diffusivity of species concentration
Pr	Prandtl number
M	Hartman number
N_b	Brownian motion parameter
N_t	thermophoresis parameter
Sc	Schmidt number
N_r	Buoyancy ratio
N_c	Bioconvection Rayleigh number

q_w	surface heat flux
h_m	surface mass flux
Nu_z	Local Nusselt number
Sh_z	local Sherwood number
Re_z	local Reynolds number
Nn_z	density number of motile microorganisms
k^*	Porous medium permeability
F	inertia coefficient of the porous medium
k_r^2	reaction rate
n	Fitted rate constant
E_a	activation energy
κ	Boltzmann constant
β_1	Porosity parameter
F_r	local inertia coefficient
σ	dimensionless reaction rate
E	dimensionless activation energy
δ	temperature difference parameter
D_n	Diffusivity of the microorganism
w_c	Constant maximum cell swimming speed
Lb	Bioconvection Lewis number
Pr	Prandtl number
Pe	Peclet number
σ_1	Bioconvection parameter
N	Density of the motile microorganisms
N_f	Constant motile microorganism
q_n	Surface motile microorganism flux
σ_e	electrical conductivity

ν	kinematic viscosity
ρ	Density
ρ_m	Density of microorganism
γ	curvature parameter
λ	mixed convection parameter
μ	Viscosity
ϕ	dimensionless fluid concentration
θ	dimensionless temperature
η	transformed coordinate
α	thermal diffusivity
τ	ratio between heat capacity
β	Casson fluid parameter
β_T	coefficient of thermal expansion
γ_1	thermal Biot number
γ_2	concentration Biot number
h_f, h_θ, h_ϕ	non-zero auxiliary parameters
L_f, L_θ, L_ϕ	linear operators
f_0, θ_0, ϕ_0	initial approximations
$c_1, c_2 \ldots c_7$	Constants

Chapter 1

Introduction and Literature review

1.1 Introduction

Nanofluids are heat transmitting fluids formed by the dispersion of nano sized particles in ordinary base fluids. The ordinary fluids usually have low thermal conductivity. Smaller channels would face hindrance if ordinary fluids that carry millimeter (mm) or nanometer (μm) sized particles are used. Nanofluids are one of the latest evaluations in the field of nano technology. Expected increase was noticed in thermal conductivity of fluid after immersing nano particles (smaller than 100 nm in diameter) in ordinary base fluid. The upgrade in thermal conductivity of nano fluid plays a vital role in many industrial applications like pharmaceuticals, micro electronics, nuclear reactors etc. The following four properties are responsible for the magnificent characteristics of nanofluids.

- Dominant temperature dependent thermal conductivity
- Intensified thermal conductivity in response of low nanoparticles concentration
- Nonlinear expansion in thermal conductivity utilizing nanoparticle
- Escalation in boiling critical heat flux.

Darcy law explains the movement of homogenous fluids through spongy media. This law was composed by Henri Darcy (a French civil engineer) after performing experiments on the flow properties of sand filters used to filter the water. As a result of these experiments he came to know that viscous forces dominate over inertial forces in spongy media, which later on known as Darcy Law. Darcy law presumes laminar fluid flow lacking the density (inertial term) which shows that absence of inertial term is not the case in classical Navier-Stokes equations. Vast surface area in a porous media is subject to fluid flow which is the basic supposition of Darcy law. This law is of great importance in the field of mechanics and used in petroleum technology, water structures and in grain stokes. Darcy law is not suitable nearby the wall because at this area permeable medium has high rate of flow. Keeping this in mind, one has to be concerned about the Non-Darcian influence by porous media in the flow analysis and rate of heat transfer. In 1901, Philippe Forcchheimer while performing the experiment on flowing gas through coal beds disclosed that there is a nonlinear relationship among potential gradient and flow rate at higher velocity. Initially, he supposed that this non linear rise is due to the turbulence in flow but it is now revealed that inertial effects in the porous media are responsible for these non-linear effects. Hence, mechanism of Forchheimer is introduced for high flow rate. The addition of quadratic term in equation of motion is introduced by Forchheimer known as Forchheimer expression. Physically, for porous media a quadratic drag in the equation of motion arises for rising filtration velocities. This drag is formed due to solid obstructs and at the surface this drag is similar to surface drag by resistance. There are several examples where Darcy law is not valid due to significant inertial effects. Hence, Darcy Forchheimer law is more suitable for the flows where the velocities are high.

In 1889, Svante Arrhenius (Swedish scientist) was the one who introduced the term activation energy. The least amount of energy needed to begin a chemical reaction is considered as activation energy and is represented by E_a. Activation energy is affected by temperature gradient and catalyst. Different reactions require different amount of activation energy so this is not same for all chemical reactions. The two type of reactions are

endothermic reaction and exothermic reaction. More energy is required for endothermic reaction while reverse situation occurred for exothermic reactions. The chemical reaction rate depends upon temperature, concentration and activation energy. There is a close relationship between rate of chemical reaction and its activation energy. Escalation in activation energy reduces the chemical reaction because few molecules can get the control over activation energy barrier to complete the reaction.

Convection is a process of heat transfer in the fluid by the movement of molecules. Diffusion and advection both are involved in this process. The process of convection is mostly used in soft solids or in fluids where the particles can easily move. There are several types of convections like natural convection, gravitational convection, Bio-convection etc. In Bio-convection process gyrotactic microorganisms are used to cause convection. Gyrotactic microorganisms are tiny living organisms which are denser than water. Bio-convection occurs due to the up swimming of motile organisms. When upper surface of the fluid becomes thick due to collection of microorganisms, it becomes unstable and they move down to causes Bio-convection. Recent evaluations in medical and industrial applications have introduced a vast variety of non-newtonian liquids which are differentiated by various deviations from the viscous fluids. Non-newtonian liquids are those for which the rate of shear can be changed but shear stress doesn't change in the same proportion. These liquids are generally divided into three categories as time dependent, viscoelastic and time independent liquids. Casson liquid is one of the Non-Newtonian fluid and has wide applications in bioengineering operations, food processing, making of pharmaceutical products and biological fluids.

1.2 Literature Review

Nano fluids are homogeneous combination of nano-particles and base fluids that have potential to transfer heat. These fluids are of much importance among researchers due to its magnified thermic conductive property and convective heat transmitting coefficient.

It is perceived that thermal conductivity of liquid is improved when we add very small quantity of nano-particles in it. The stream which is complying with productive relation of Casson fluid is initiated by stretched cylinder. The fluid stream over a stretching cylinder is of much significance because of its significant applications for instance drawing of plastic movies, glass fiber, and paper creation and so forth. In mixed convection flows buoyancy forces enhances due to differences in temperature and concentration. Mixed convection flow is of much significance because of its significant applications including atomic reactors chilled during crises shutoff, electronic appliances chilled by fans and so forth. The mixed convection flows in addition with heat and mass transfer are significant in engineering that comprises energy from polymer and metal sheets [1-9].

The boundary layer stream of Casson fluid past a vertical exponential stretched barrel is studied by Malik et al. [10] while the hydromagnetic Casson fluid flow with the effects of magnification in radiation over the stretched cylinder is considered by Ramesh et al. [11]. Non Newtonian materials does not possess linear association between stress and deformation tensor. These materials are of much importance in technological and industrial processes. Differential, integral and rate are the three categories of non Newtonian fluids. The plastic liquids which possess shear stress in constitutive equations is called Casson fluid. Some Casson fluid examples are jam, tomato sauce, soup, meals processing, artificial lubricants, paints, coal in water , sewage sludge and human blood Hayat et al. [12].

In 1901, Forchheimer extend the Darcian velocity articulation by including the square of velocity terms in energy condition to foresee the conduct of dormancy and limit layer stream since when inertial and limit impacts happen at high stream rate, the Darcy law can't function admirably [13]. The "Forchheimer term" which is true for high Reynolds number was later named by Muskat [14]. Rashid et al. [15] discussed the Darcy Forchheimer effect on the motion of maxwell fluid past an exponential surface with activation and thermic radiant energy. Rashid et al.[16] also claimed that due to stretching cylinder entropy is initiated in Darcy forchheimer flow stream of nanofluid

while nanofluid contains aluminum oxide, silver, copper oxide, titanium oxide and copper as nanoparticles in it. The activation energy and mixed convection properties in Darcy forchheimer nano-meter stream by compact chamber were inspected by Waqas et al. [17]. The Darcy-Forchheimer 3D nanofluid flow model with activation energy past the rotating frame under the influence of chemical reaction is deliberated by Hayat et al. [18]. Saeed et al. [19] investigates the thermal properties of Darcy forchheimer fluid flow through stretched cylinder and the fluid is hydromagnetic hybrid nanofluid.

Activation energy and chemical reaction along with mass shift process is used in various fields for example in chemical engineering, processing of food, mechanics of oil and water fusion, geothermal reservoirs etc. First of all, the flow of binary mixture in a spongy media along with natural convection and activation energy was discussed by Bestman. Some more recent investigations in this direction were made in which Maleque worked on activation energy along with exothermic/endothermic reactions on mixed convection flows,whereas Abbas et al. explored numerically the impact of activation energy on a chemical reaction which is involved in the movement of casson fluid [20-23]. In the existence of eolotropic slip, binary chemical reaction and activation energy, the numerical treartment of radiative nano-fluid three-dimensional flow containing gyrotactic microorganisms was analysed. Some recognizable discoveries of this research are that, on the compactness of motile microorganisms, the slip parameter has an increasing effect. For dimensionless activation energy, there is decline in local density number of microorganisms against Schmidt number, dianchin et al. [24]. Huang and C.J. [25] considered the porous horizontal cylinder and discussed the effects of activation energy on free convection.

The solidity of adjournment of gyrotectic micro-organisms depends on the permeability of the porous media in a system of super imposed fluids and porus layers, however this dependence is crucial only if the fluid layer is comparatively thin compared to the porous layer [26]. The base liquid thickness is upgraded by motile microorganism a specific way so that they cause the Bio-convection stream [27]. Hussain et al.

[28] studied the impact of heat generation/absorption and thermic radiations on the squeezing nano-fluid flow. The fluid is flowing between two aligned plates from which one plate is considered fixed and other is stretching plate. Microorganisms can survive only in water so water is taken as base fluid. The porous medium implanted in a casson type non-newtonian fluid was observed with the help of protracted form of Darcy Forchheimer model and to examine 2-D steady laminar MHD incompressible flow past an exponential shrinking sheet, the impact of slip condition and viscous dissipation is applied. The result of this study shows that to obtain the solution, strong mass suction was required when forchheimmer parameter increases [29]. Rashad et al. [30] worked on motile microorganisms with convective boundary condition over a circular cylinder in mixed Bio-convection nano fluid flow. Bhatti et al. [31] worked on MHD nanofluid flow stream using motile microorganisms along with the effect of chemical reaction and thermal radiation. Chemical reaction and non linear thermal emission in a MHD nanofluid flow along motile microorganisms are discussed by Ramzan et al. [32]. Alsaedi et al. [33] worked on bioconvection phenomenon generated by gyrotactic microorganisms in a MHD nanofluid flow. Microorganisms are helpful in biomicrosystems as they take part in mass transmitting process and mixing. Furthermore, thermal conductivity is enhanced by nanofluids. The rate of heat transfer is considerably high when nanofluid is merged with motile gyrotactic microorganisms [34-38].

The prime objective of the present study is to scrutinized the casson nanofluid flow over a nonlinear stretched cylinder under Darcy- Forchheimer porous medium. Moreover, the novelty of the presented problem is improved by the addition of activation energy and motile gyrotactic microorganisms. None of the above quoted and even existing literature simultaneously analyzed such effects. Numerical solution of the problem is acquired by utilizing bvp4c built-in function of MATLAB scheme.

Chapter 2

Preliminaries

This section contains standard definitions, concepts and basic laws which are useful in understanding the works in the subsequent chapters.

2.1 Fluid

A substance that is able to flow and can change its shape under the effect of shear stress is defined as fluid. Some of its examples are water, air, honey and blood .

2.1.1 Fluid mechanics

The branch of science which concerns about the behavior of fluid at rest or in motion. The subclasses of fluid mechanics are:

2.1.2 Fluid statics

It concerns with the properties of liquids at rest.

2.1.3 Fluid dynamics

It concerns with the properties of liquids in the state of motion.

2.2 Flow

Flow is specified as a material that deforms smoothly under the effect of various kinds of forces. Flow is further divided into two major subclasses.

2.2.1 Laminar flow

Laminar flow is an orderly flow of fluid particles in regular paths or in adjacent surfaces without jumbling with each other.

2.2.2 Turbulent flow

In turbulent flow the fluid experiences irregular variations and the fluid velocity at a point is continuously changes in the flow field.

2.3 Viscosity

Viscosity is the measure of fluid resistance to flow when various forces are acting on it. It is also interpreted as the internal friction of fluid.

$$\text{viscosity } = \frac{\text{shear stress}}{\text{gradient of velocity}}. \tag{2.1}$$

2.3.1 Dynamic viscosity

It measures the fluid resistance to it's motion. Its unit is kg/ms.

2.3.2 Kinematic viscosity

Kinematic viscosity is described as fluid absolute viscosity divided to density of fluid. It is represented by

$$\nu = \frac{\mu}{\rho} = \frac{\text{absolute viscossity}}{\text{fluid density}}, \tag{2.2}$$

In SI system unit is $\frac{m^2}{s}$.

2.4 Newtonian fluids

The fluids whose viscosity at all shear rates remains the same is considered as Newtonian fluids. In these fluids the gradient of velocity (du)/(dy) and shear force $\boldsymbol{\tau}_{yx}$ is linearly proportional to each other. some examples of this fluid are water, kerosene Alcohol and glycerine.

2.5 Non-Newtonian fluids

Fluids whose viscosity does not remain same at all shear rates or that does not satisfy the Newton's law of viscosity. Here, shear stress has non linear and direct relation with and velocity gradient. Mathematicaly, it can be represented as:

$$\boldsymbol{\tau}_{yx} \propto \left(\frac{du}{dy}\right)^n, \ n \neq 1, \tag{2.3}$$

or

$$\boldsymbol{\tau}_{yx} = \eta \frac{du}{dy}, \ \eta = s\left(\frac{du}{dy}\right)^{n-1}, \tag{2.4}$$

where η is named as apparent viscosity, $\boldsymbol{\tau}_{yx}$ is shear stress, s shows consistency index and the flow behaviour index is defined by n. For $n = 1$, Eq. (2.4) represents the Newton law of viscosity. Yougurt, honey and ketchup shows the non-Newtonian fluid behavior.

2.6 Newton viscosity law

In Newton law of viscosity, shear rate and shear force has linear correspondence. Mathematically, it can be represented as follows:

$$\tau_{yx} \propto (\frac{du}{dy}), \tag{2.5}$$

or

$$\tau_{yx} = \mu \left(\frac{du}{dy} \right), \tag{2.6}$$

in which τ_{yx} indicates the shear force which act on the fluid element and μ indicate the proportionality constant.

2.7 Density

Density is obtained by dividing the mass of material by its volume. Mathematical representation of density is:

$$\rho = \frac{m}{V}, \tag{2.7}$$

where m is the mass of material and V is the volume. Unit of density in SI system is kg/m^3.

2.8 Pressure

The perpendicular force applied on a surface of an object divided by unit area is termed as pressure.

Mathematically pressure is given by:

$$P = \frac{F}{A}, \tag{2.8}$$

In SI system, Nm^{-2} is defined as the unit of pressure.

2.9 Porous surface

The surface which contains pores or empty spaces from which fluid or gas can penetrate. Paper, sponge, ceramics and fabrics are some examples of porous surface.

2.10 Porosity

Porosity is specified as the measure of empty spaces in a porous medium.

2.11 Permeability

The property of permeable material which allows the fluid to penetrate through it is known as permeability.

2.12 Mechanism of heat flow

The transfer of thermal energy occurs when there is temperature difference between the surfaces. Heat flows from colder surface to hotter surface. The heat transfer takes place through following three ways:

2.12.1 Conduction

In the phenomenon of conduction, heat energy is transmitted from higher to lower temperature area through the vibration of atoms and molecules. Mathematically

$$\frac{\boldsymbol{q}}{A} = k\frac{\Delta T}{\Delta X} \quad = \quad k\left(\frac{T_1 - T_2}{X_1 - X_2}\right), \tag{2.9}$$

where

$$\boldsymbol{q} = -kA\frac{dT}{dx}, \tag{2.10}$$

in which $\boldsymbol{q}$ represents the heat flow, A represents surface area, k the thermal conductivity, T_2 temperature is smaller than T_1 , $\frac{dT}{dx}$ denotes the temperature gradient and negative sign shows that heat is conducted from higher to lower temperature.

2.12.2 Radiation

A phenomenon in which heat reaches to cold temperature region from hot temperature region because of waves is called radiation. Mathematically

$$\boldsymbol{q} = e\sigma^{**} A \left(\Delta T\right)^4, \tag{2.11}$$

where $\boldsymbol{q}$ denotes the heat transfer, e for emissivity of the system, σ^{**} for Stephen-Boltzmann constant, A for area and $(\Delta T)^4$ for the temperature difference between two systems of fourth power.

2.12.3 Convection

A phenomenon where transfer of heat takes place due to the motion of molecules from high temperature gradient to low temperature gradient is known as convection. Mathematically

$$q = hA \left(T_s - T_\infty\right), \tag{2.12}$$

where h is coefficient of heat transfer (convective), T_s for system temperature, A for area and T_∞ for the ambient temperature.

2.13 Convective boundary condition

The condition in which transfer of heat through the vibration of molecules (conduction) is equal to the transfer of heat due to the motion of molecules (convection) is said to be convective boundary conditions. These kind of conditions are usually define on wall (surfaces). Mathematically

$$k \left(\frac{\partial T}{\partial r_i}\right)_{x_i} = h[T_f(x_i, t) - T\ (x_i, t)], \tag{2.13}$$

where h indicates the coefficient of heat transfer (convective) , x_i is the coordinate at the boundary, T_f the convective fluid temperature and T represents wall temperature.

2.14 Nanofluid

The fluid that can be formed by assembling the nanometer particles with base fluid is called nano fluid. It amplifies the thermal conductivity of the mixture. The nano sized particles used in Nanofluid are mostly oxides, metal or nanotubes. Oil and water are commonly used base fluids.

2.15 Casson Nanofluid

Casson fluid falls in the group of non-Newtonian liquids which is considered as shear thinning liquid. This fluid is supposed to have infinite shear rate at zero viscosity and zero shear rate at an infinite viscosity. An appropriate example of Casson fluid is human blood.

2.16 Darcy Law

Flow of liquid through permeable media is explained by Darcy law. This law was derived and depends upon the outcome of examination on the flow of water across the sand beds.

2.17 Darcy Forchheimer Law

Forchheimer term is the additional inertial term in Darcy equation. This inertial term arises from porous medium flow where flow has prominent inertial effects with Reynolds numbers greater than 10. The non-linear conduct of pressure difference against flow data is described by this term.

$$\frac{\partial p}{\partial x} = \frac{\mu}{k^*}\upsilon_f - \frac{\rho}{k_1}\upsilon_f^2, \tag{2.14}$$

where k_1 represents inertial permeability and υ_f represents Forchheimer velocity.

2.18 Activation Energy

The base energy required for a chemical response to happen is known as activation energy. This energy depends upon its rate, if the energy is low then the reaction rate is high or vice versa.

2.19 Gyrotectic Microorganisms

These are the motile microorganisms that exist in oceans, lakes and rivers. Gyrotectic microorganisms are used in experiments as they help in Bio-convection. When large number of microorganisms assembles on the upper layer of suspension, the layer becomes dense and the microorganisms become unstable and start moving towards down, this results in Bio-convection.

2.20 Non-dimensional numbers

2.20.1 Reynolds number (Re)

The ratio of forces of inertia to viscous forces is described by Reynolds number. It is a dimensionless number and used to identify the laminar or turbulent flow behaviour of fluid. Mathematically, this number is expressed as:

$$\mathrm{Re} = \frac{\text{Forces of inertia}}{\text{Viscous forces}}, \tag{2.15}$$

$$= \frac{v \times l}{\nu}, \tag{2.16}$$

Here, v defines the fluid velocity, l defines characteristic length and ν describes kinematic viscosity. Flow shows turbulence at high Reynolds number when Re is greater than 2100

while the flow is laminar at low Reynolds number when Re is less or equal to 2100.

2.20.2 Prandtl number (Pr)

Momentum diffusivity to thermal diffusivity ratio is named as Prandtl number . Mathematically, Prandtl number can be interpret as

$$\mathrm{Pr} = \frac{\nu}{\alpha}, \tag{2.17}$$

$$\mathrm{Pr} = \frac{\mu c_p}{k}, \tag{2.18}$$

where μ shows the dynamic viscossity, the specific heat is denoted by c_p and k represents thermal conductivity.

2.20.3 Peclet number (Pe)

Peclet number is interpreted as a ratio of transfer of thermal energy by fluid movement to transfer of thermal energy by diffusion.

$$Pe = \frac{\text{advective tranfer rate}}{\text{diffusive tranfer rate}}. \tag{2.19}$$

Peclet number is a dimensionless number.

2.20.4 Nusselt number (Nu_z)

The ratio of heat shift through convection to heat shift through conduction at the boundary is defined by dimensionless number known as Nusselt Number. Mathematical representation is

$$Nu_z = \frac{h\Delta T}{k\Delta T/l} = \frac{hl}{k}, \tag{2.20}$$

where h interprets heat transmitting coefficient (convective), characteristic length is denoted by l and k represents thermal conductivity.

2.20.5 Biot number (γ_1)

It is a dimensionless number which defines the relation among heat transfer resistance inside the body and heat transfer resistance on the surface. Mathematically, it is represented as follows:

$$\gamma_1 = \frac{hl}{k}, \tag{2.21}$$

where k represents the thermal conductivity and h shows heat shift coefficient (convective) .

2.20.6 Thermophoresis parameter (Nt)

Thermophoresis helps to split different particles from mixture after combining due to the existence of temperature gradient or it stops different particles to combine with each other due to pressure gradient.

Hot surface has negative while the cold surface has positive thermophoresis.

Mathematically

$$Nt = \frac{(\rho c)_p D_T (T_f - T_\infty)}{(\rho c)_f \ \nu T_\infty}, \tag{2.22}$$

where T_f and T_∞ denotes the convective fluid temperature and ambient temperature respectively, D_T represents thermophoretic coefficient and ν shows kinematic viscosity.

2.20.7 Brownian motion parameter (Nb)

The random movement of suspended microscopic particles occurs due to their bumping with high velocity molecules is known as Brownian motion. Mathematically

$$Nb = \tau \frac{D_B (C_f \ - C_\infty)}{\nu}, \tag{2.23}$$

in the above equation τ is the ratio of effective heat and heat capacity of the nanoparticles and fluid respectively, v denotes the kinematic viscosity. C_f stands for fluid concentration, C_∞ stands for ambient concentration and D_B represents Brownian diffusion coefficient.

2.20.8 Schmidt number (Sc)

Kinematic viscosity divided by Brownian diffusion cofficient is denoted by dimensionless number known as Schmidt number. Mathematically

$$Sc = \frac{\nu}{D_B}, \tag{2.24}$$

where ν shows kinematic viscosity and D_B is Brownian diffusion cofficient.

2.20.9 Forchheimer number (Fr)

Pressure gradient to the viscous resistance ratio is described by forchheimer number.

Mathematically

$$Fr = \frac{k^* \rho \nu \beta^*}{\mu}, \tag{2.25}$$

with β^*non-Darcian coefficient and $k^*$the permeability of porous medium.

2.20.10 Sherwood number (Sh)

This number describes the ratio among convective mass transfer and the mass transfer through diffusion

$$\text{Sh}=\frac{h}{d \ / \ l}, \tag{2.26}$$

where h shows convective mass transfer rate and d represents diffusivity and l is characterstic length.

2.21 Conservation law

A measurable quantity that remains constant with the progression of time in an isolated system is known as conserved quantity and the law which deals with this quantity is defined as conservation law. The conservation laws that are used for the flow specification in the subsequential analysis are given below.

2.21.1 Mass conservation law

Mass conservation law describes that the whole mass in any closed system will remain conserved. Mathematically

$$\frac{D\rho}{Dt} + \rho(\boldsymbol{\nabla}.(\mathbf{V})) = 0, \tag{2.27}$$

or

$$\frac{\partial\rho}{\partial t} + (\mathbf{V}.\boldsymbol{\nabla})\,\rho + \rho\boldsymbol{\nabla}.\mathbf{V} = 0, \tag{2.28}$$

or

$$\frac{\partial\rho}{\partial t} + \boldsymbol{\nabla}.\,(\rho\mathbf{V}) = 0, \tag{2.29}$$

The above equation is known as equation of continuity. For the steady flow Eq. (2.32) becomes

$$\boldsymbol{\nabla}.\,(\rho\mathbf{V}) = 0, \tag{2.30}$$

and for the incompressible fluid, Eq. (2.33) will be stated as:

$$\boldsymbol{\nabla}.\mathbf{V} = 0. \tag{2.31}$$

2.21.2 Momentum conservation law

The total linear momentum of a closed system is constant is defined as momentum conservation law. Generally, it is given by

$$\rho \frac{D\mathbf{V}}{Dt} = \operatorname{div} \boldsymbol{\tau} + \rho \mathbf{b}, \tag{2.32}$$

where ($\boldsymbol{\tau} = -\mathbf{pI} + \mathbf{S}$) the Cauchy stress tensor, $\frac{D}{Dt}$ is appeared as the material time derivative and $\mathbf{b}$ stands for body force.

2.21.3 Law of energy conservation

The total energy is conserved at the whole system is said to be law of conservation of energy and this law is also known as energy equation. For nanofluids it is specified by

$$\rho_f c_f \frac{DT}{Dt} = \tau^* . L^* + k\nabla^2 T + \rho_p c_p \left(D_B \nabla C . \nabla T + \frac{DT}{T_\infty} \nabla T . \nabla T \right), \tag{2.33}$$

in which ρ_f represents the density of base fluid, c_f stands for specific heat of base fluid, τ^* the stress tensor, L^* for the strain tensor, ρ_p denotes the density of nanoparticles, D_B indicates the Brownian diffusivity, D_T represents the thermophoretic diffusion coeffiecient, k denotes the thermal conductivity and T for temperature.

2.21.4 Concentration conservation law

For nanoparticles, the volume fraction equation is

$$\frac{\partial C}{\partial t} + \mathbf{V} . \boldsymbol{\nabla} \mathbf{C} = -\frac{1}{\rho_p} \boldsymbol{\nabla} . \mathbf{j}_p \ , \tag{2.34}$$

$$\mathbf{j}_p = -\rho_p D_B \nabla C - \rho_p D_T \frac{\nabla T}{T_\infty}, \tag{2.35}$$

$$\frac{\partial C}{\partial t} + \mathbf{V}.\boldsymbol{\nabla}\mathbf{C} = \mathbf{D}_B\boldsymbol{\nabla}^2\mathbf{C} + \mathbf{D}_T\frac{\boldsymbol{\nabla}^2 T}{T_\infty}. \tag{2.36}$$

Here, D_B, C, T and D_T stand for Brownian diffusivity, nanoparticle concentration, temperature and thermophoretic coefficients respectively.

2.22 Thermal diffusivity

It is a material specific property for describing the unsteady conductive heat flow. This value describes how speedily a material respond to change in temperature. It is the ratio of thermal conductivity to specific heat capacity of fluid. Mathematically,

$$\alpha = \frac{k}{(\rho c)_f}, \tag{2.37}$$

where the thermal conductance is denoted by k , $(\rho c)_f$ the capacity of specific heat.

2.23 Thermal conductivity

It is the measurement of the capacity of a material to conduct heat. The Fourier law of heat conduction " The amount of heat transfer rate (q) through a material of unit thickness (d) times unit cross section area (A) and unit temperature difference (ΔT)". Mathematically, written as:

$$k = \frac{qd}{A(\Delta T)}. \tag{2.38}$$

In SI system thermal conductivity has unit $\frac{W}{m.K}$.

2.24 Homotopic solutions

Homotopy is one of the basic concept of topology. It is stated as continous mapping in which one function can be constantly transformed into the another function. If one function h_1 and the other h_2 are maps from the topological space D with the other topological space E, then there exists a continous mapping H such that

$$H : D \times [0\ , 1] \rightarrow E, \tag{2.39}$$

where $d \in D$ and

$$F(d, 0) = h_1(x), \tag{2.40}$$

$$F(d, 1) = h_2(x). \tag{2.41}$$

That mapping H is termed as homotopy.

2.25 Homotopy Analysis method

The Homotopy Analysis method (HAM) is involved to find the series solutions of highly nonlinear problems. This method presents us with convergent series solutions for highly nonlinear systems.

Chapter 3

Mixed convection flow of Casson nanofluid past a stretched cylinder with convective boundary conditions

In this chapter, we consider the mixed convection Casson fluid flow induced by stretched cylinder with convective heat and mass conditions in addition with nano sized particles. The nonlinear partial differential system is reduced to ordinary differential system by applying appropriate transformations. Homotopy analysis method (HAM) is applied to obtain the convergent solution of the system.

3.1 Mathematical formulation

In this chapter, we consider an incompressible, Casson nanofluid flow bounded by stretched cylinder with convective boundary conditions. The existence of magnetic field does not effect the fluid electric conductivity. In radial direction, r-axis is deliberated while alongside the axis of cylinder, z-axis is taken into consideration (Figure 3.0). The uniform magnetic field whose intensity is denoted by B_0 is assumed to be in the radial direction. Here, u and w are velocities, u along $z-$ direction and w along $r-$ direction. T is

temperature of fluid and C is fluid concentration. Similarly, T_∞ represents the ambient temperature and C_∞ represents the ambient concentration.

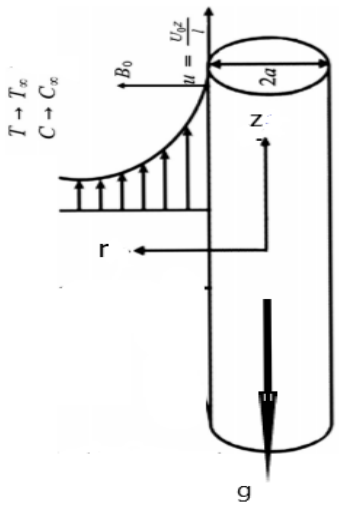

Fig 3.0: Problem

Geometery

The governing equations are:

$$\frac{\partial u}{\partial z} + \frac{w}{r} + \frac{\partial w}{\partial r} = 0, \tag{3.1}$$

$$u\frac{\partial u}{\partial z} + w\frac{\partial u}{\partial r} = \nu\left(1 + \frac{1}{\beta}\right)\left(\frac{\partial^2 u}{\partial r^2} + \frac{1}{r}\frac{\partial u}{\partial r}\right)$$

$$+g\left[\beta_T\left(T - T_\infty\right)\left(1 - C_\infty\right) + \frac{\left(\rho^* - \rho\right)}{\rho}\left(C - C_\infty\right)\right] - \frac{\sigma_e B_0^2 u}{\rho}, \tag{3.2}$$

$$u\frac{\partial T}{\partial z} + w\frac{\partial T}{\partial r} = \alpha\left(\frac{\partial^2 T}{\partial r^2} + \frac{1}{r}\frac{\partial T}{\partial r}\right) + \tau\left[D_B\frac{\partial T}{\partial r}\frac{\partial C}{\partial r} + \frac{D_T}{T_\infty}\left(\frac{\partial T}{\partial r}\right)^2\right], \tag{3.3}$$

$$u\frac{\partial C}{\partial z} + w\frac{\partial C}{\partial r} = D_B\left(\frac{\partial^2 C}{\partial r^2} + \frac{1}{r}\frac{\partial C}{\partial r}\right) + \frac{D_T}{T_\infty}\left(\frac{\partial^2 T}{\partial r^2} + \frac{1}{r}\frac{\partial T}{\partial r}\right), \tag{3.4}$$

with the boundary conditions

$$u = U = \frac{U_0 z}{l},\ v = 0,\ -k\frac{\partial T}{\partial r} = h\ (T_f - T)\,,$$

$$-D_m\frac{\partial C}{\partial r} = k_m\ (C_f - C)\ \text{at}\ \ \text{r = a},$$

$$u \to 0,\ T \to T_\infty\ , C \to C_\infty \text{ as } r \to \infty. \tag{3.5}$$

Dimensionless form of above mathematical model is derived by using following transformations:

$$u = z\ \frac{U_0}{l} f\ '(\eta)\,, \quad w = -\frac{1}{r}\sqrt{\frac{U_0\nu}{l}} a\ f\ \ (\eta)\,,$$

$$\psi = (U\nu z)^{\frac{1}{2}}\ a\ f\ \ (\eta)\,,\ \ \eta = \frac{r^2 - a^2}{2a}\sqrt{\frac{U}{\nu z}},$$

$$\theta(\eta) = \frac{T - T_\infty}{T_f - T_\infty}, \qquad \phi\,(\eta) = \frac{C - C_\infty}{C_f - C_\infty}\ , \tag{3.6}$$

Here, satisfaction of Eq. (3.1) is inevitable. However, Eqs.(3.2) − (3.5) reduce to

$$\left(1 + \frac{1}{\beta}\right)[(1 + 2\gamma\eta)\, f''' + 2\gamma f''] + ff'' - f\ '^2 + \lambda\,(\theta + N_r\phi) - Mf\ ' = 0, \tag{3.7}$$

$$\frac{1}{\Pr}\left[(1 + 2\gamma\eta)\,\theta'' + 2\gamma\theta^{'}\right] + f\ \theta' + Nb\,(1 + 2\gamma\eta)\,\theta'\phi' + Nt\,(1 + 2\gamma\eta)\,\theta^{'^2} = 0, \tag{3.8}$$

$$(1 + 2\gamma\eta)\,\phi'' + 2\gamma\phi' + Scf\ \phi' + \frac{Nt}{Nb}\left[(1 + 2\gamma\eta)\,\theta'' + 2\gamma\theta^{'}\right] = 0, \tag{3.9}$$

$$f(0) = 0,\ f'(0) = 1,\ \theta^{'}(0) = -\gamma_1\,(1 - \theta\,(0))\,,\ \phi'\,(0) = -\gamma_2\,(1 - \phi\,(0))\,, \tag{3.10}$$

$$f'(\infty) = 0, \quad \theta\,(\infty) = 0, \quad \phi(\infty) = 0, \tag{3.11}$$

with

$$\gamma = \sqrt{\frac{\nu l}{U_0 a^2}},\ \lambda = \frac{g l^2 \beta_T}{U_0^2 z}\,(1 - C_\infty)\,(T_f - T_\infty)\,,\ Nt = \frac{\tau D_T\,(T_f - T_\infty)}{\nu T_\infty},$$

$$Nr = \frac{(\rho^* - \rho)\,(C_f - C_\infty)}{\rho\beta_T\,(T_f - T_\infty)\,(1 - \phi_\infty)},\ M = \frac{\sigma_e\ B_0^2 l}{\rho U_0},\ Nb = \frac{\tau D_B\,(C_f - C_\infty)}{\nu},$$

$$\mathrm{Pr} = \frac{\nu}{\alpha},\ Sc = \frac{\nu}{D_B},\ \gamma_1 = \frac{h}{k}\sqrt{\frac{\nu l}{U_0}},\ \gamma_2 = \frac{k_m}{D_m}\sqrt{\frac{\nu l}{U_0}}. \tag{3.12}$$

The local Nusselt number and local sherwood number are

$$Nu_z = \frac{zq_w}{k\left(T_f - T_\infty\right)}, \qquad Sh_z = \frac{zh_m}{D_B\left(C_f - C_\infty\right)} \tag{3.13}$$

where the wall heat flux q_w and the wall mass flux h_m are defined as

$$q_w = -k\frac{\partial T}{\partial r}|_{r=a}, \qquad h_m = -\ D_B\frac{\partial C}{\partial r}|_{r=a} \tag{3.14}$$

The local Nusselt number and local sherwood number in dimensionless quantities by using equations (3.13) and (3.14) are appended as follows:

$$Nu_z\left(\mathrm{Re}_z\right)^{-1/2} = -\theta'\left(0\right), \tag{3.15}$$

$$Sh_z\left(\mathrm{Re}_z\right)^{-1/2} = -\phi'\left(0\right). \tag{3.16}$$

Reynolds number is given as, $\mathrm{Re}_z = \frac{Uz}{\nu}$

3.2 Solutions procedure

Homotopy analysis method is used to find the solution of system. It is an analytical method applied to compute the convergent series solutions. This method discriminates itself from other analytical techniques because of some important attributes.

Following this method, the initial guess $\left[f_0\left(\eta\right), \theta_0\left(\eta\right), \phi_0\left(\eta\right)\right]$ and relevant linear operators $(\mathrm{L}_f\ , \mathrm{L}_\theta,\ \mathrm{L}_\phi)$ are expressed below:

$$f_0\left(\eta\right) = \left[1 - \exp\left(-\eta\right)\right],$$

$$\theta_0\left(\eta\right) = \left(\frac{\gamma_1}{1+\gamma_1}\right)\exp\left(-\eta\right), \qquad \phi_0\left(\eta\right) = \left(\frac{\gamma_2}{1+\gamma_2}\right)\exp\left(-\eta\right), \tag{3.17}$$

$$\mathrm{L}_f \ = f\,''' - f\,',\ \mathrm{L}_\theta \ = \theta'' - \theta,\ \mathrm{L}_\phi \ = \phi'' - \phi, \tag{3.18}$$

along with the properties

$$\mathrm{L}_f\left[c_1 + c_2\exp(\eta) + c_3\exp(-\eta)\right] = 0,$$

$$\mathrm{L}_\theta[c_4\exp(\eta) + c_5\exp(-\eta)] = 0,$$

$$\mathrm{L}_\phi[c_6\exp(\eta) + c_7\exp(-\eta)] = 0, \tag{3.19}$$

here c_j and $(j = 1 - 7)$ are defined as optional constants.

3.3 Convergence analysis

Homotopy analysis method is applied to find the convergence solution of system of non linear equations which depends upon supplementary variables $\hbar_f$, $\hbar_\theta$ and $\hbar_\phi$. These variables are important to adjust and manage the convergence zone while plotting h–curves. The admissible ranges of $\hbar_f$, $\hbar_\theta$ and $\hbar_\phi$ are $-1.1 \leq \hbar_f \leq -0.5$, $-1.4 \leq \hbar_\theta \leq -0.2$ and $-1.3 \leq \hbar_\phi \leq -0.4$. Table 3.1 represents the series solution convergence and it displays that 30^{th} order of guesstimate is enough to establish the series solution. It can be noticed that the values from table are adequately in order to the h- curves shown in Fig. 3.1.

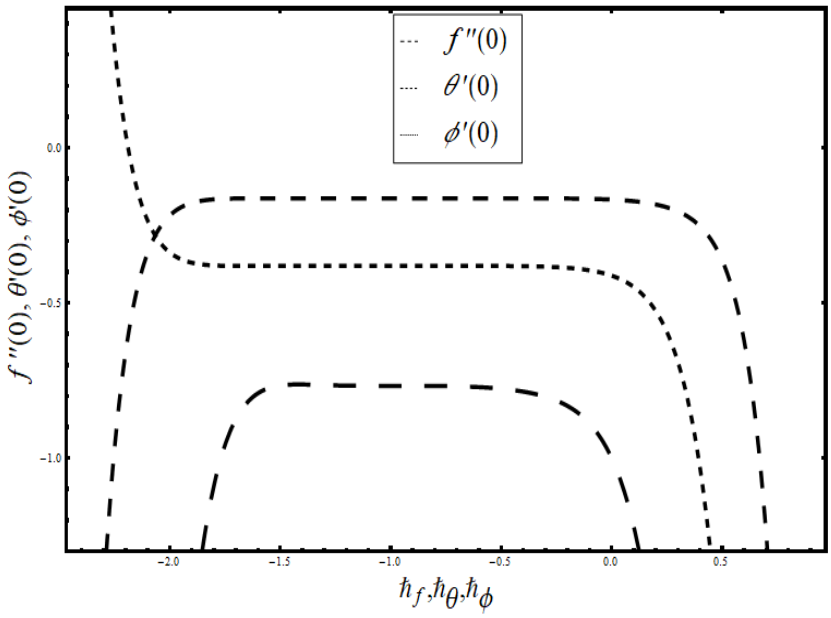

Figure 3.1: h-curves for f, θ and ϕ

Table 3.1**:** Convergence of Homotopy series solutions for varied order of estimations.

Order of Approximation	$-f''(0)$	$-\theta'(0)$	$-\phi'(0)$
1	0.87552	0.15903	0.31705
5	0.82354	0.15542	0.28887
10	0.82498	0.15572	0.28845
15	0.82495	0.15570	0.28858
20	0.82493	0.15570	0.28856
25	0.82493	0.15570	0.28856
30	0.82493	0.15570	0.28856

3.4 Results and discussion

This section examines the impacts of distinct variables on all involved distributions through graphical illustrations.

Figure 3.2 is framed to show the impact of β the casson fluid parameter on velocity field $f'(\eta)$. Graph portrays that velocity is a dwindling function of β. The reason is that resistance is produced in the fluid motion due to increasing values of β and this resistance suppresses the velocity and eventually velocity reduces. Figure 3.3 illustrates that how curvature parameter γ affects the velocity $f'(\eta)$. In fact the fluid flow is showing an amplifying behavior on increasing values of curvature parameter γ. By increasing this parameter, the radius of cylinder enhances and this cause an increase in velocity feild. Impact of mixed convection parameter λ on fluid velocity $f'(\eta)$ is appeared in Figure 3.4. The parameter λ is expressed as mixed convection parameter. By increasing this parameter, the buoyancy forces escalate. The escalation in buoyancy forces results in increase of velocity profile. Figure 3.5 depicts that rising values of Nr put escalating effect on the fluid velocity $f'(\eta)$. The increasing values of Nr increases the force of convection between molecules which causes the thickness of momentum boundary layer and hence velocity increases. Graph 3.6 displays the impact of M the Hartman number on fluid velocity. This parameter M is expressed as the ratio between electromagnetic forces to viscous force. By increasing this parameter, the magnetic field enhances and produces resistive force which is responsible for the reduction in velocity profile.

Impact of temperature variation $\theta(\eta)$ against curvature parameter γ can be viewed in Fig 3.7. It can be visualaized that increasing values of curvature parameter γ give rise to temperature. This is due to the fact that by increasing the cylinder curvature, the velocity of fluid rises resulting in enhancement of kinetic energy. As Kelvin temperature is described as an average kinetic energy, so when kinetic energy increases temperature also increases. Figure 3.8 is sketched to describe the effect of Brownian motion parameter Nb on the temperature profile $\theta(\eta)$. The rise in Brownian motion parameter enhances the random movement of nano size particles due to which kinetic energy is generated and

rapid collision between particles take place. Due to bumping of particles kinetic energy is transformed into heat energy and therefore temperature rises. Impact of thermophoresis variable Nt on fluid temperature $\theta(\eta)$ can be seen in Fig 3.9. The temperature is showing an increase on growing estimates of Nt. When thermophoretic force enhances due to enhancement in Nt, the nanoparticles start moving from hot region to cold region and this cause a rise in fluid temperature. Figure 3.10 displays that there is rise in temperature $\theta(\eta)$, on rising values of thermal Biot number γ_1. This is due to the fact that escalating estimates of Biot number enhances the heat transmitting coefficient which cause a rise in fluid temperature $\theta(\eta)$ as well as in thermal boundary layer thickness.

Figure 3.11 shows the effect of curvature parameter γ on concentration $\phi(\eta)$. The concentration ϕ and associated boundary layer enhances due to enhancement in curvature parameter. Figure 3.12 displays that how the concentration profile $\phi(\eta)$ is effected by Brownian motion variable Nb. For rising value of Nb, the fluid concentration diminishes. It is perceived that with rise in Nb random monement of macroscopic fluid particles and collision among themselves increase which helps to heat up the boundary layer and ultimately the concentration of the fluid decreases. The impact of thermophoresis variable Nt upon concentration distribution $\phi(\eta)$ can be seen in Figure 3.13. An increase in concentration field is observed against gradual escalation in Nt. The reason behind is that on increasing the values of Nt the variation between ambient temperature and surface temperature enhances which cause a rise in fluid concentration. Fig 3.14 illustrates the impact of Schmidt number Sc on fluid concentration $\phi(\eta)$. As Schmidt number is a ratio of viscosity to mass diffusivity, the rise in Sc reduces the mass diffusivity which in turns cause a depletion in fluid concentration ϕ. The impact of concentration Biot number γ_2 on volume fraction $\phi(\eta)$ is depictied in graph 3.15. It is noted that the rising values of concentration biot number causes upsurge in the fluid concentration. This is due to the fact that escalating estimates of Biot number enhances the mass transmission which cause a rise in fluid concentration.

Table 3.2 is drawn to show the impact of curvature parameter γ, Brownian motion

parameter Nb, thermophoresis motion parameter Nt, thermal Biot number (γ_1) and concentration Biot number (γ_2) on Nusselt and on Sherwood numbers. It is noted that for greater estimates of Nb, Nt, γ_2 the value of Nusselt number $[Nu_z\,(\mathrm{Re}_z)^{-\frac{1}{2}}]$ decreases while it enhances for increasing values of γ and γ_1. The Sherwood number $[Sh_z\,(\mathrm{Re}_z)^{-1/2}]$ diminishes by escalating Nt and γ_1 while it enhances for increasing values of Nb, γ, and γ_2.

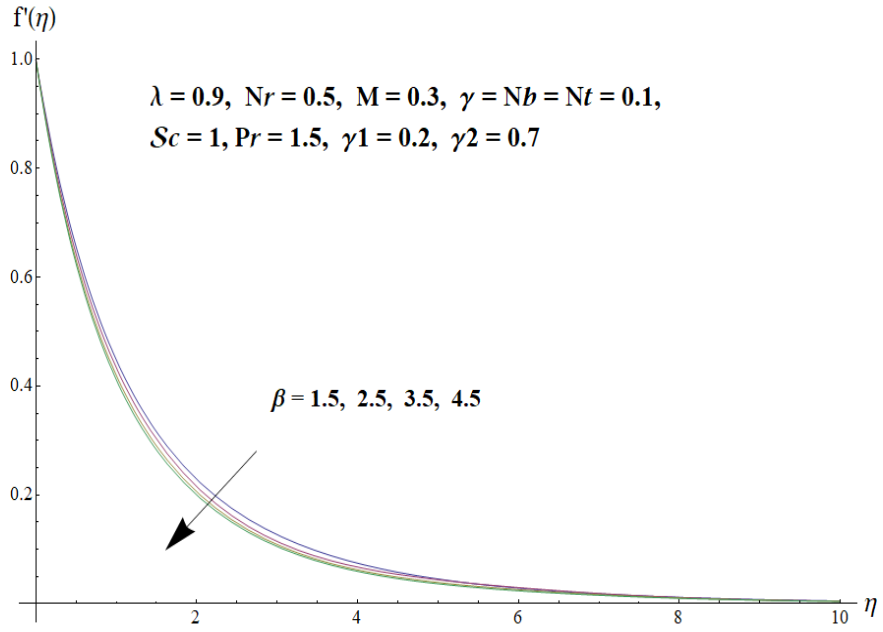

Figure 3.2: Effect of β on $f'(\eta)$

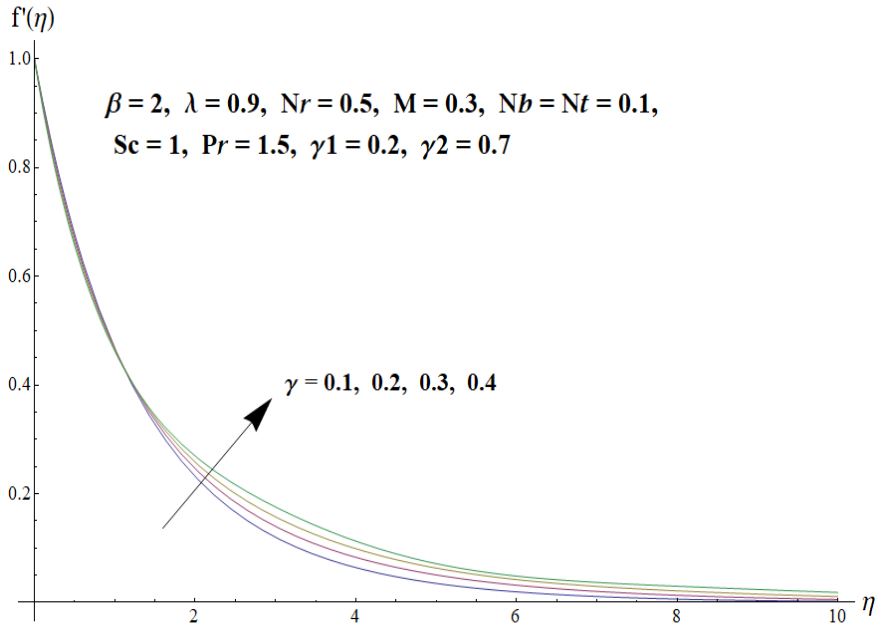

Figure 3.3: Effect of γ on $f'(\eta)$

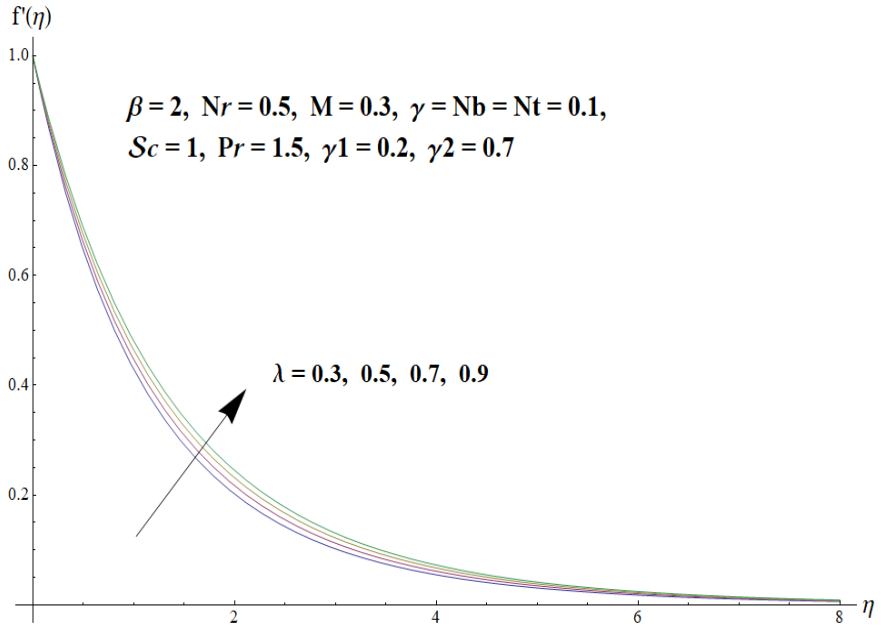

Figure 3.4: Effect of λ on $f'(\eta)$

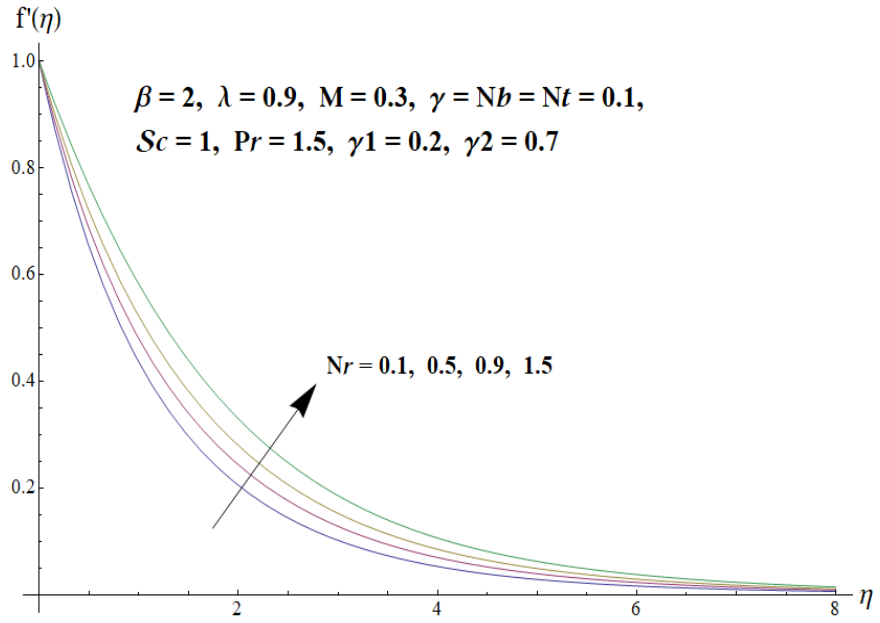

Figure 3.5: Effect of Nr on $f'(\eta)$

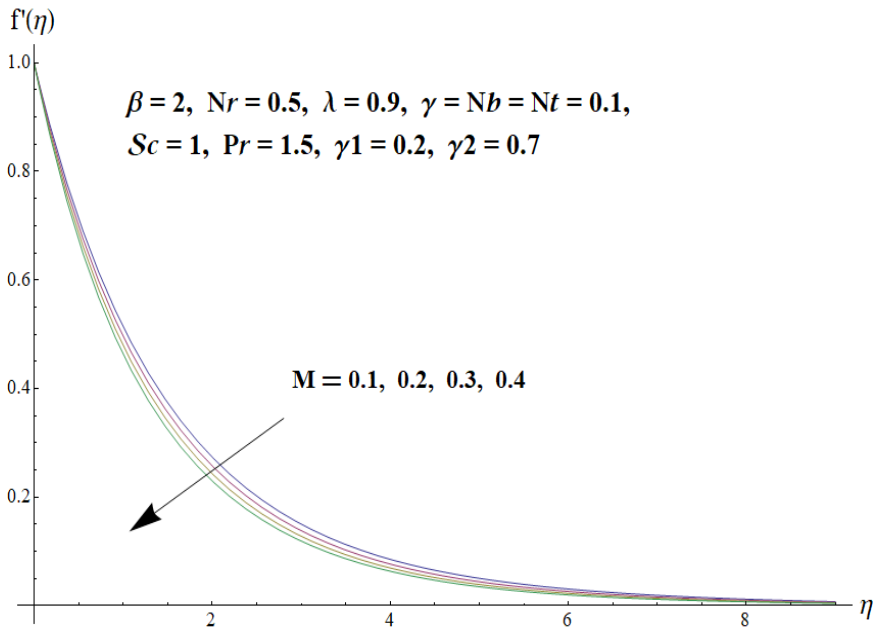

Figure 3.6: Effect of M on $f'(\eta)$

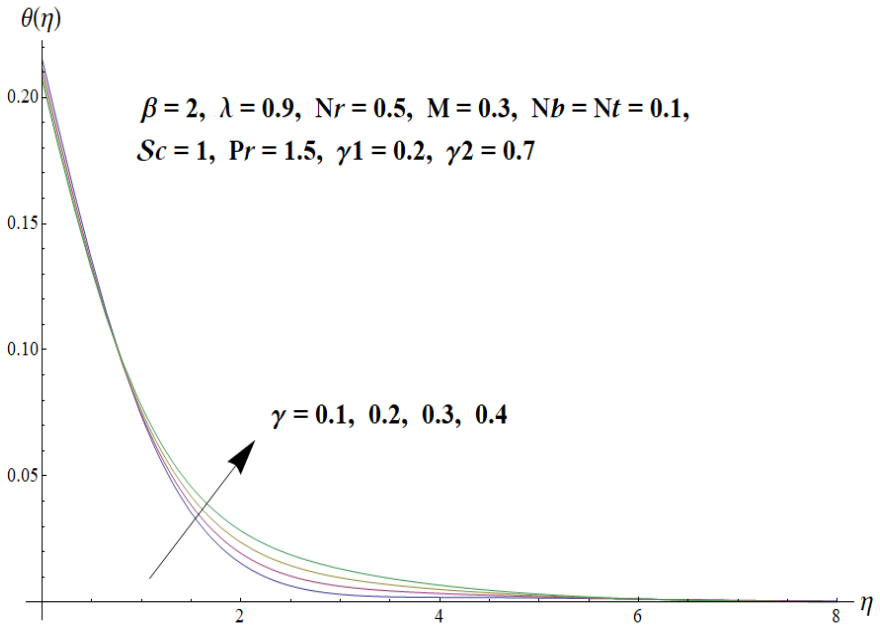

Figure 3.7: Effect of γ on $\theta(\eta)$

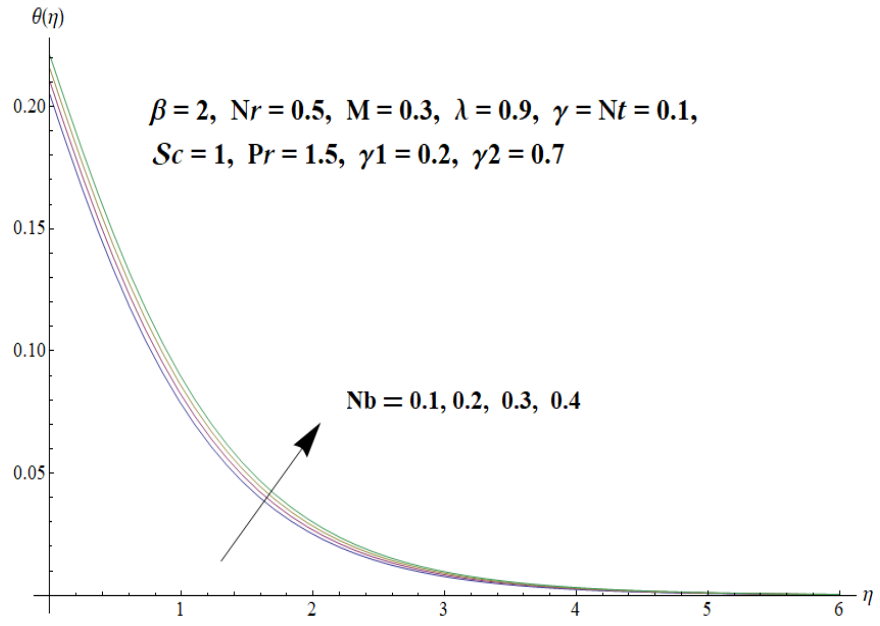

Figure 3.8: Effect of Nb on $\theta(\eta)$

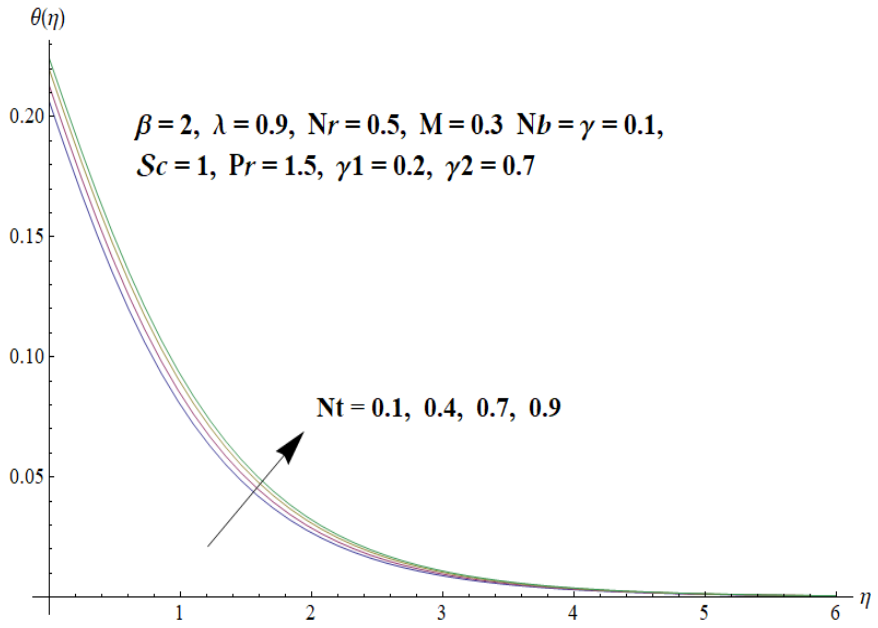

Figure 3.9: Effect of Nt on $\theta(\eta)$

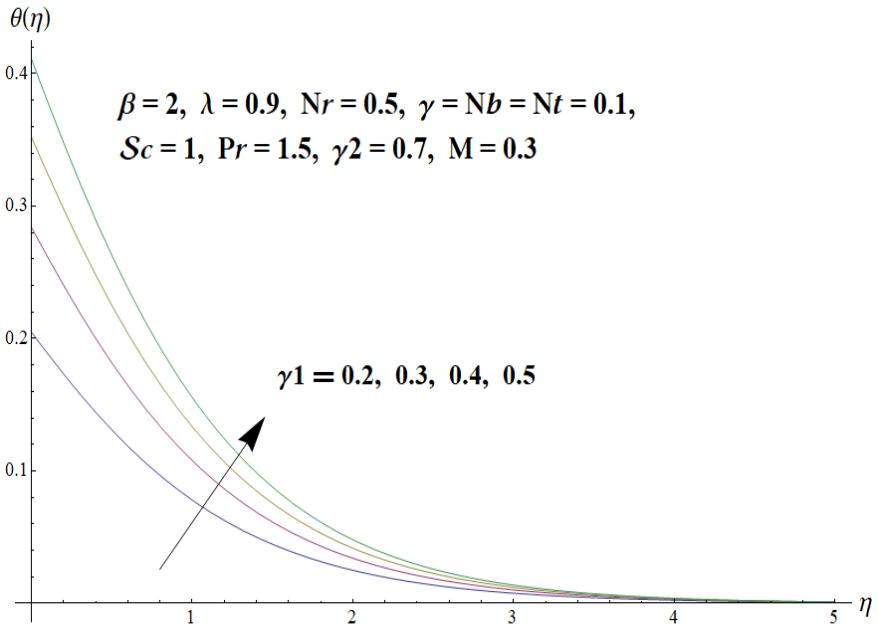

Figure 3.10: Effect of γ_1 on $\theta(\eta)$

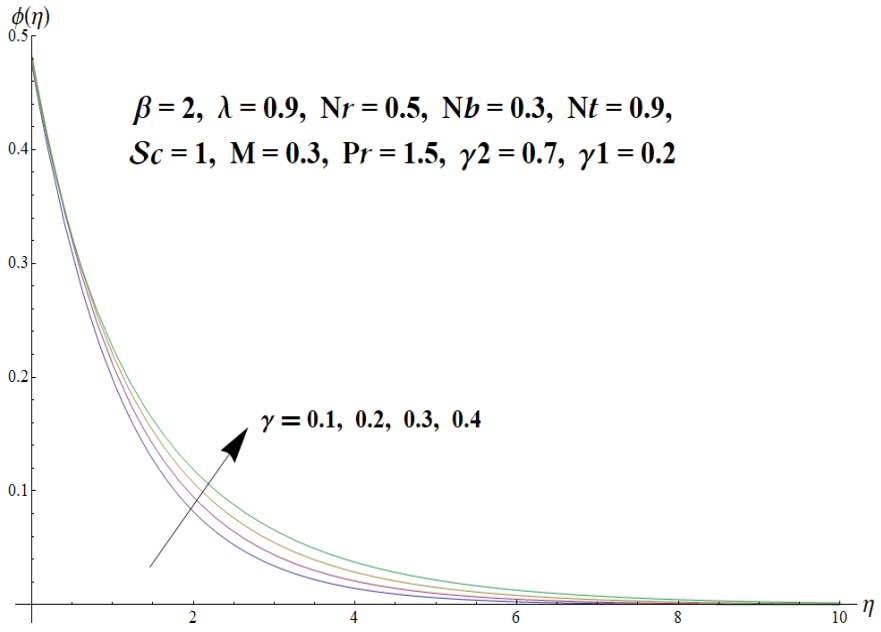

Figure 3.11: Effect of γ on $\phi(\eta)$

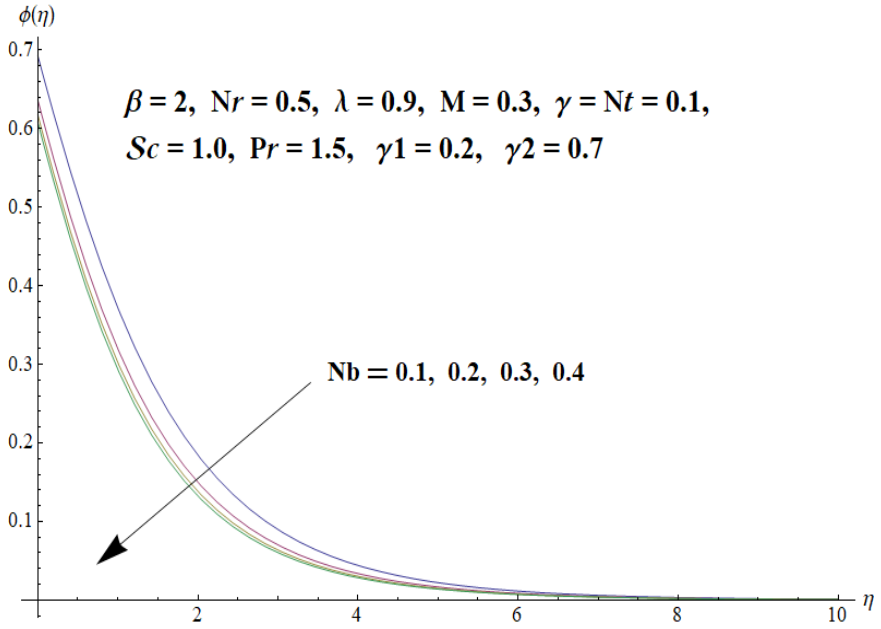

Figure 3.12: Effect of Nb on $\phi(\eta)$

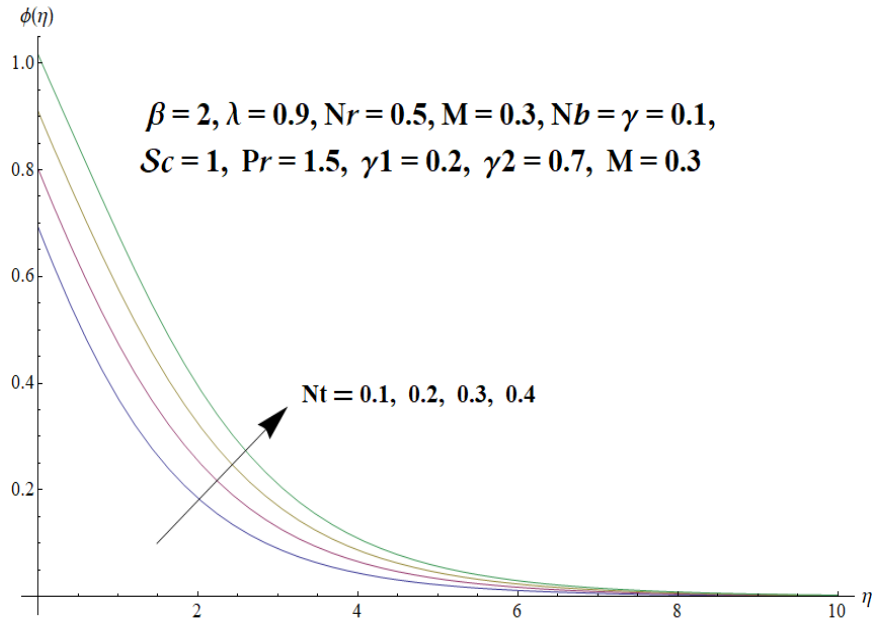

Figure 3.13: Effect of Nt on $\phi(\eta)$

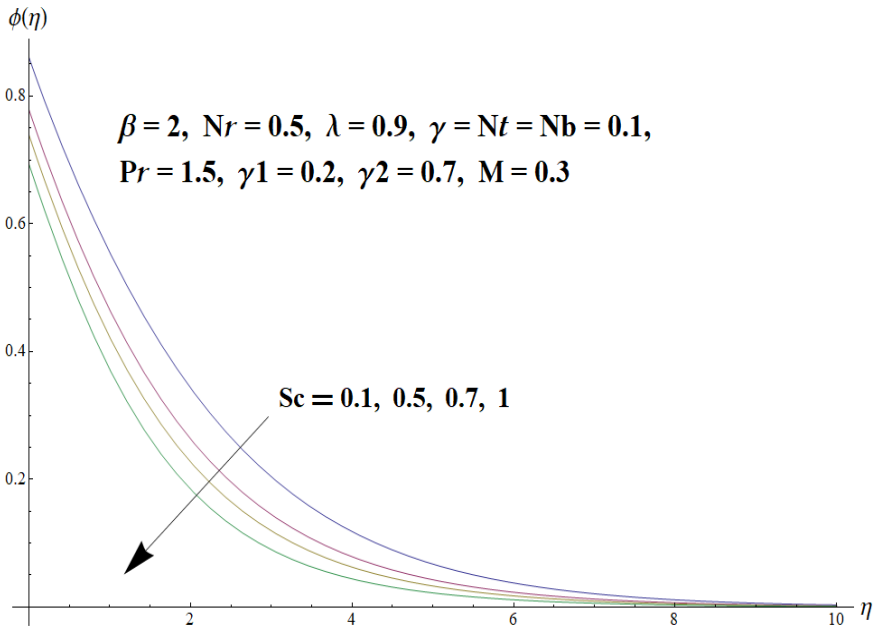

Figure 3.14: Effect of Sc on $\phi(\eta)$

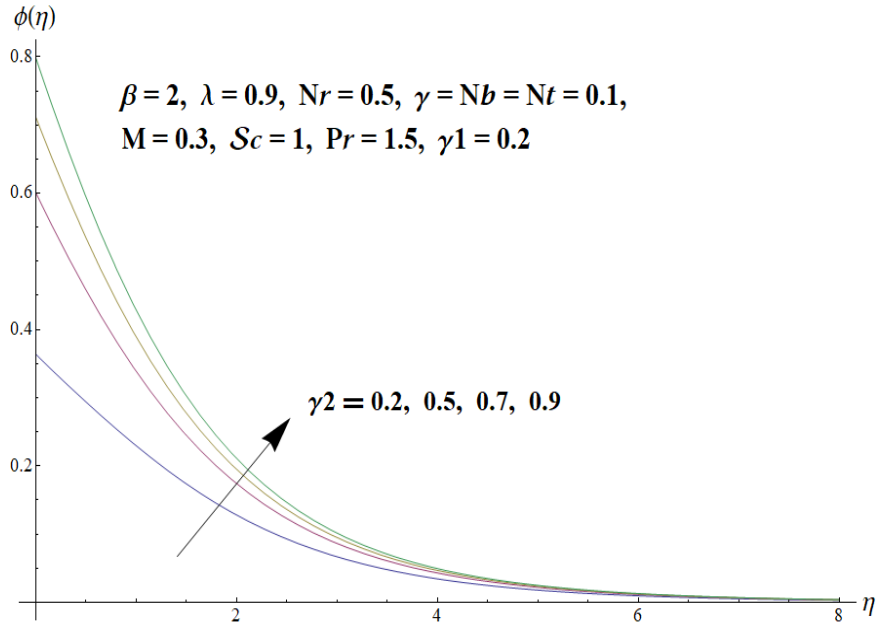

Figure 3.15: Effect of γ_2 on $\phi(\eta)$

Table 3.2: Numeric values of Nusselt and Sherwood numbers.

γ	Nb	Nt	γ_1	γ_2	$Nu_z\,(\mathrm{Re}_z)^{-\frac{1}{2}}$	$Sh_z\,(\mathrm{Re}_z)^{-\frac{1}{2}}$
0.1	0.1	0.1	0.2	0.7	0.15571	0.28856
0.2					0.15712	0.29877
0.3					0.15839	0.30942
0.1	0.2				0.15459	0.31332
	0.3				0.15352	0.32173
	0.4				0.15243	0.32602
	0.1	0.2			0.15553	0.24168
		0.3			0.15532	0.19622
		0.4			0.15513	0.15235
		0.1	0.5		0.29332	0.25090
			0.7		0.35292	0.23510
			0.9		0.39792	0.22329
			0.2	0.5	0.15578	0.24135
				0.8	0.15569	0.30742
				1.0	0.15563	0.33836

Chapter 4

Darcy–Forchheimer Casson nanofluid flow over a stretching cylinder with Arrhenius activation energy and gyrotactic microorganisms

In this chapter, Casson fluid flow is studied in Darcy-Forchheimer porous medium with activation energy and gyrotactic microorganisms. The nonlinear partial differential system is reduced to ordinary differential system by applying appropriate transformations. Built in function bvp4c (MATLAB) is used to obtain the convergent solution of the system.

4.1 Mathematical modelling

In this chapter we consider a Darcy–Forchheimer Casson nano-fluid flow over a stretched cylinder along with Arrhenius activation energy and gyrotactic microorganisms.The $z-$axis

is deliberated alongside the axis of cylinder while $r-$axis is taken along radial direction with respective velocities u and w (Figure 4.0).The flow is supported by the convective mass and heat transfer boundary conditions.

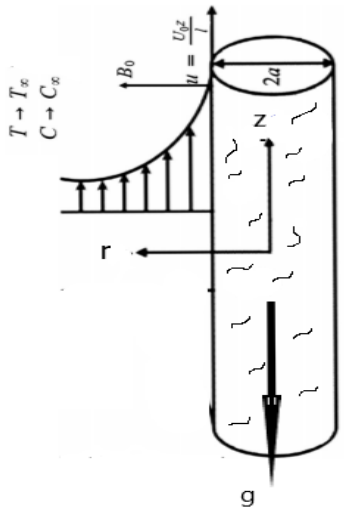

Fig 4.0: Problem

Geometery

The governing system representing the given scenario is given as:

$$\frac{\partial u}{\partial z} + \frac{w}{r} + \frac{\partial w}{\partial r} = 0, \tag{4.1}$$

$$u\frac{\partial u}{\partial z} + w\frac{\partial u}{\partial r} = \nu\left(1 + \frac{1}{\beta}\right)\left(\frac{\partial^2 u}{\partial r^2} + \frac{1}{r}\frac{\partial u}{\partial r}\right) - \frac{\sigma_e B_0^2 u}{\rho} - \frac{\nu}{k^*}u - Fu^2$$

$$+g\left[\beta_T\left(\mathrm{T} - \mathrm{T}_\infty\right)\left(1 - C_\infty\right) + \frac{\left(\rho^* - \rho\right)}{\rho}\left(C - C_\infty\right) - \gamma\left(N - N_\infty\right)\left(\frac{\rho_m - \rho}{\rho}\right)\right], \tag{4.2}$$

$$u\frac{\partial \mathrm{T}}{\partial z} + w\frac{\partial \mathrm{T}}{\partial r} = \alpha\left(\frac{\partial^2 \mathrm{T}}{\partial r^2} + \frac{1}{r}\frac{\partial \mathrm{T}}{\partial r}\right) + \tau\left[D_B\frac{\partial \mathrm{T}}{\partial r}\frac{\partial C}{\partial r} + \frac{D_T}{T_\infty}\left(\frac{\partial \mathrm{T}}{\partial r}\right)^2\right], \tag{4.3}$$

$$u\frac{\partial C}{\partial z}+w\frac{\partial C}{\partial r}=D_B\left(\frac{\partial^2 C}{\partial r^2}+\frac{1}{r}\frac{\partial C}{\partial r}\right)+\frac{D_T}{T_\infty}\left(\frac{\partial^2 T}{\partial r^2}+\frac{1}{r}\frac{\partial T}{\partial r}\right)$$
$$-k_r^2\left(C-C_\infty\right)\left(\frac{T}{T_\infty}\right)^n\exp\left(-\frac{E_a}{\kappa T}\right), \tag{4.4}$$

$$u\frac{\partial N}{\partial z}+v\frac{\partial N}{\partial r}=D_n\left(\frac{\partial^2 N}{\partial r^2}+\frac{1}{r}\frac{\partial N}{\partial r}\right)-\frac{d\ w_c}{C_f-C_\infty}\ \frac{\partial}{\partial r}\left(N\frac{\partial C}{\partial r}\right). \tag{4.5}$$

supported by the boundary conditions

$$u=U=\frac{U_0 z}{l},\ v=0,-k\frac{\partial T}{\partial r}=h\ \left(T_f-T\right),$$

$$-D_m\frac{\partial C}{\partial r}=k_m\ \left(C_f-C\right),\ N=N_f\ \text{at}\ \ \text{r = a},$$
$$u\to 0,\ T\to T_\infty\ ,C\to C_\infty,\ N\to N_\infty\ \text{as}\ r\to\infty. \tag{4.6}$$

Dimensionless form of above mathematical model is acquired by using following transformations:

$$u=z\ \frac{U_0}{l}f\ '\left(\eta\right),\ w=-\frac{1}{r}\sqrt{\frac{U_0\nu}{l}}a\ f\ \ \left(\eta\right),$$

$$\psi=\left(U\nu z\right)^{\frac{1}{2}}\ a\ f\ \ \left(\eta\right),\qquad \eta=\frac{r^2-a^2}{2a}\sqrt{\frac{U}{\nu z}},$$
$$\theta(\eta)=\frac{T-T_\infty}{T_f-T_\infty},\quad \phi\left(\eta\right)=\frac{C-C_\infty}{C_f-C_\infty}\ ,\quad \chi\left(\eta\right)=\frac{N-N_\infty}{N_f-N_\infty}, \tag{4.7}$$

Here, satisfaction of Eq. (4.1) is inevitable. However, Eqs. $(4.2)-(4.6)$ becomes:

$$\left(1+\frac{1}{\beta}\right)\left[\left(1+2\gamma\eta\right)f'''+2\gamma f''\right]+ff''-f\ '^2+\lambda\left[\theta+N_r\phi-N_c\chi\right]$$
$$-Mf\ '-\beta_1 f\ '-F_r\ f\ '^2=0, \tag{4.8}$$

$$\frac{1}{\mathrm{Pr}}\left[\left(1+2\gamma\eta\right)\theta''+2\gamma\theta'\right]+f\ \theta'+Nb\left(1+2\gamma\eta\right)\theta'\phi'+Nt\left(1+2\gamma\eta\right)\theta'^2=0, \tag{4.9}$$

$$\left(1+2\gamma\eta\right)\phi''+2\gamma\phi'+Scf\ \phi'+\frac{Nt}{Nb}\left[\left(1+2\gamma\eta\right)\theta''+2\gamma\theta'\right]$$
$$-Sc\sigma\left(1+\delta\theta\right)^n\phi\exp\left(-\frac{E}{1+\delta\theta}\right)=0, \tag{4.10}$$

$$(1+2\gamma\eta)\,\chi'' + 2\gamma\chi' + Lb\ \Pr f\ \chi'$$

$$-Pe\left[(1+2\gamma\eta)\,\phi'\chi' + \gamma\chi\phi' + (1+2\gamma\eta)\,\phi'' + \sigma_1\gamma\phi' + \sigma_1\,(1+2\gamma\eta)\,\phi''\right] = 0, \tag{4.11}$$

$$f(0) = 0, f\,'(0) = 1,\ \theta'(0) = -\gamma_1\,(1-\theta(0))\,, \phi'(0) = -\gamma_2\,(1-\phi(0))\,, \chi(0) = 1, \tag{4.12}$$

$$f'(\infty) \to 0,\ \theta(\infty) \to 0,\ \phi(\infty) \to 0,\ \chi(\infty) \to 0. \tag{4.13}$$

with

$$\gamma = \sqrt{\frac{\nu l}{U_0 a^2}},\quad \lambda = \frac{gl^2\beta_T}{U_0^2 z}\,(1-C_\infty)\,(T_f - T_\infty)\,,\quad Nt = \frac{\tau D_T\,(T_f - T_\infty)}{\nu T_\infty}, M = \frac{\sigma_e\ B_0^2 l}{\rho U_0},$$

$$Nr = \frac{(\rho^* - \rho)\,(C_f - C_\infty)}{\rho\beta_T\,(T_f - T_\infty)\,(1-\phi_\infty)},\ Nc = \frac{\gamma\,(\rho_m - \rho)\,(N_f - N_\infty)}{\rho\beta_T\,(T_f - T_\infty)\,(1-C_\infty)},\ Nb = \frac{\tau D_B\,(C_f - C_\infty)}{\nu},$$

$$\Pr = \frac{\nu}{\alpha},\ Sc = \frac{\nu}{D_B},\ \gamma_1 = \frac{h}{k}\sqrt{\frac{\nu l}{U_0}},\ \gamma_2 = \frac{k_m}{D_m}\sqrt{\frac{\nu l}{U_0}},\ \beta_{1=}\frac{vl}{U_0 k^*},\ \delta = \frac{T_f - T_0}{T_\infty},$$

$$E = \frac{E_a}{\kappa T_\infty},\ F_r = \frac{C_b}{k^{*1/2}},\ \sigma = \frac{k_r^2 l}{U_0},\ Lb = \frac{\alpha}{D_n},\ Pe = \frac{dw_c}{D_n},\ \sigma_1 = \frac{N_\infty}{N_f - N_\infty}. \tag{4.14}$$

where Local Nusselt number, local sherwood number and density number of motile microorganisms are

$$Nu_z = \frac{zq_w}{k\,(T_f - T_\infty)},\quad Sh_z = \frac{zh_m}{D_B\,(C_f - C_\infty)},\quad Nn_z = \frac{zq_n}{D_n \Delta N}. \tag{4.15}$$

where the wall heat flux q_w, the wall mass flux h_m and surface motile microorganisms flux q_n are given as

$$q_w = -k\frac{\partial T}{\partial r}|_{r=a},\quad h_m = -\ D_B\frac{\partial C}{\partial r}|_{r=a},\quad q_n = -\ D_n\frac{\partial N}{\partial r}|_{r=a}\ . \tag{4.16}$$

Local Nusselt number, local sherwood number and density number of motile microor-

ganisms in dimensionless form is defined as follows:

$$Nu_z \left(\mathrm{Re}_z\right)^{-1/2} = -\theta'(0), \tag{4.17}$$

$$Sh_z \left(\mathrm{Re}_z\right)^{-1/2} = -\phi'(0), \tag{4.18}$$

$$Nn_z \left(\mathrm{Re}_z\right)^{-1/2} = -\chi'(0). \tag{4.19}$$

$\mathrm{Re}_z = \frac{Uz}{\nu}$ expresses the local Reynolds number.

4.2 Results and discussion

This section is devoted to visualize the impact of different physical variables, on the velocity $f'(\eta)$, temperature $\theta(\eta)$, concentration fields $\phi(\eta)$ and on density of motile microorganisms $\chi(\eta)$ Figures 4.1 and 4.2 are plotted to notice the impact of fluid parameter β and curvature parameter γ on the fluid velocity $f'(\eta)$. It is witnessed that the velocity is decreasing and escalating function of β and γ respectively. Since due to increase in β the resistance produces in the fluid motion, which ultimately reduces the velocity. Whereas, by increasing γ, velocity increses, this is because of that radius of cylinder enhances by increasing the values of curvature parameter γ. The effect of Forchheimer number on the fluid velocity is plotted in Figure 4.3. It is noticed that velocity $f'(\eta)$ is diminishing function of Fr. This is because, resistance is produced in a fluid flow due to escalating values of Fr. The influence of porosity number β_1 on the velocity distribution $f'(\eta)$ is depicted in Fig 4.4. The growing estimates of porosity parameter reduce the fluid velocity. This is because the porous medium hinders the motion of fluid and this result in diminishing of velocity. Fig 4.5 depicts the effects of bioconvection Rayeigh number N_c on velocity profile $f'(\eta)$. It is observed that velocity decays by increasing Rayeigh number. Bioconvection Rayleigh number involves density difference which creates a reduction in the velocity field. Figure 4.6 and 4.7 are framed to show the impact of Brownian motion variable Nb and thermophoresis number Nt on the temperature profile $\theta(\eta)$ respectively.

The increase in Nb enhances the random movement of nano size particles, therefore rapid collision of particles started and due to which kinetic energy is transformed into heat energy. Hence temperature rises due to rise in Nb. However, the temperature is also showing an increasing behavior on escalating values of Nt. This is because an escalation in Nt enhances thermophoretic force due to which nanoparticles start moving from hot surface to cold surface. Hence, fluid temperature rises. Figure 4.8 discribes the trend of thermal Biot number γ_1 against temperature $\theta(\eta)$. On increasing estimates of thermal Biot number the heat transmitting coefficient increases which cause a rise in the fluid temperature $\theta(\eta)$ and thermal boundary layer thickness. Graph 4.9 is plotted to show the impact of activation energy E on fluid concentration $\phi(\eta)$. It is experimented that increasing estimates of activation energy puts the rising effect on concentration. The increase in activation energy decays the modified Arrhenius function due to which concentration and productive chemical reaction enhances. Graph 4.10 displays the impact of concentration profile $\phi(\eta)$ against Brownian motion variable Nb. It is noticed that the fluid concentration has dwindled due to escalation in Brownian motion variable. Actually increasing estimates of Nb speeds up the movement of fluid particles due to which boundary layer temperature increases and fluid concentration reduces. Figure 4.11 is formulated to show the trend of Schmidt number Sc against the concentration field $\phi(\eta)$. The Schmidt number has an inverse relation with mass diffusivity. When Sc enhances the mass diffusivity diminishes which in turn reduces the concentration profile. Figure 4.12 is portrayed to depict the effect of curvature parameter γ on the density of gyrotactic organisms $\chi(\eta)$. It is noticed that an increase in curvature parameter (γ) enhances the density of gyrotactic organisms $\chi(\eta)$. The increase in curvature parameter decreases the radius of cylinder and this cause a rise in density of motile microorganisms. Fig 4.13 is sketched to show how the Hartman number M affects the density of motile microorganisms $\chi(\eta)$. It is perceived that density of motile microorganisms $\chi(\eta)$ has rising effects on increasing values of M. The increase in M produces a resistance due to which density of motile microorganisms escalates. Graph 4.14 portrays the trend of Peclet number Pe on

the motile microorganisms profile $\chi(\eta)$. Pe is defined as $\frac{\mu\ L}{\delta^*}$, in which δ^* is mass diffusivity. The rise in Peclet number decreases the microorganisms diffusivity which in turns cause a down fall in motile microorganisms profile. Figures 4.15 and 4.16 are sketched to interpret the relation between the Brownian motion parameter Nb, bioconvection Lewis number Lb and the density of motile microorganisms. $\chi(\eta)$. It is perceived that motile microorganisms density diminishes for increasing values of Nb. Actually escalating values of Nb enhances the rapid movement of microorganisms that cause a rise in temperature and decline in motile microorganisms profile. However, Bioconvection Lewis number Lb is described as a ratio of thermal diffusivity to mass diffusivity. The increase in Lb reduces the mass diffusivity due to which density of motile microorganisms turns down. Graph 4.17 is sketched to portray the influence of bioconvection constant σ_1 on density of motile microorganisms $\chi(\eta)$. The enhancement in bioconvection constant augments the microorganisms concentration and reduces the motile density profile. The behavior of Prandtl number Pr against the motile microorganisms profile is illustrated in Fig 4.18. Prandtl number is explained as momentum to thermal diffusivity. By increasing Pr, the momentum diffusivity dominates and hence density of motile microorganisms $\chi(\eta)$ diminishes.

Table 4.1 shows the values of Nusselt number $Nu_x \operatorname{Re}_x^{\frac{-1}{2}}$ for different parameters. Nusselt number exhibits an decreasing behaviour on rising estimates of Nb, Nt, γ_2 while increasing behaviour is seen for γ and γ_1. Table 4.2 displays the impact of $Nt,\ Nb, \gamma_2, \gamma\ and\ E$ on sherwood number $Sh_x \operatorname{Re}_x^{\frac{-1}{2}}$. Sherwood number shows an increasing behaviour on increasing amount of Nb, γ_2, γ while decreasing behaviour is seen for Nt and E. Table 4.3 is formed to forsee the influences of $\gamma,\ M,\ Nb, Lb, Pe, \Pr$ and σ_1 on density number of motile microorganisms $Nn_x \operatorname{Re}_x^{\frac{-1}{2}}$. Density number enhances on increasing values of $\gamma,\ \Pr, Pe, Nb, Lb, \sigma_1$ while diminishes for M.

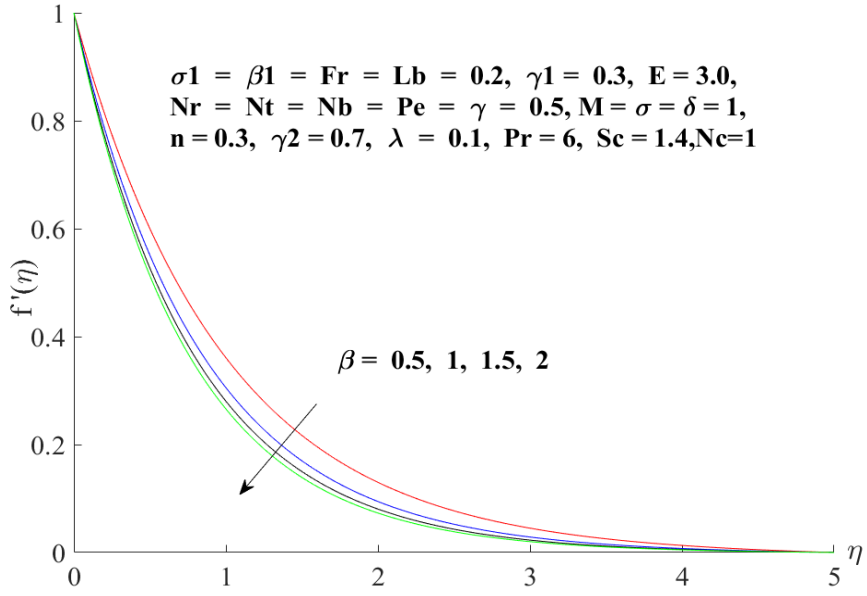

Figure 4.1: Effect of β on $f'(\eta)$

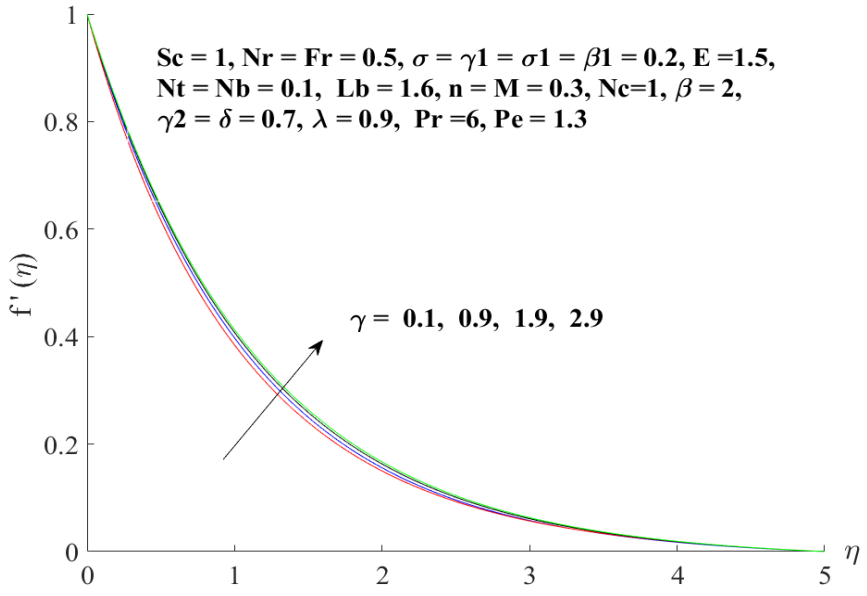

Figure 4.2: Effect of γ on $f'(\eta)$

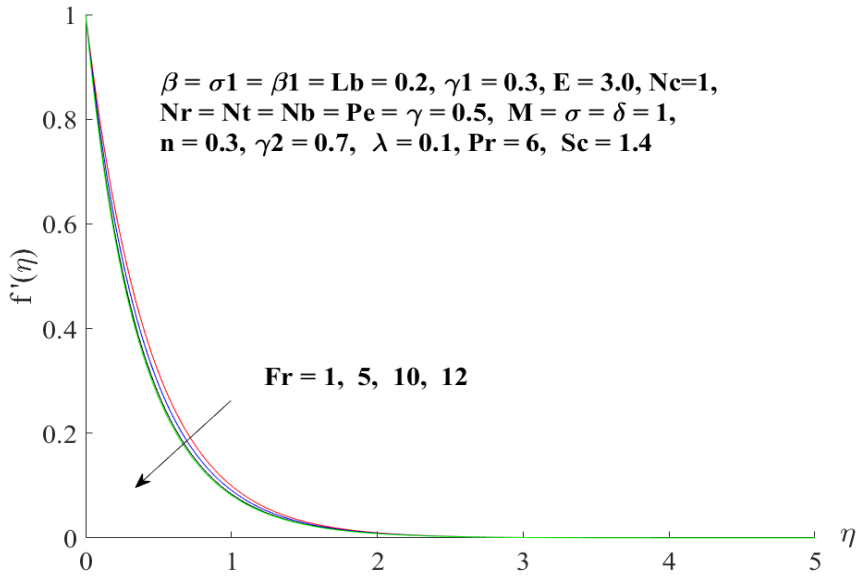

Figure 4.3: Effect of Fr on $f'(\eta)$

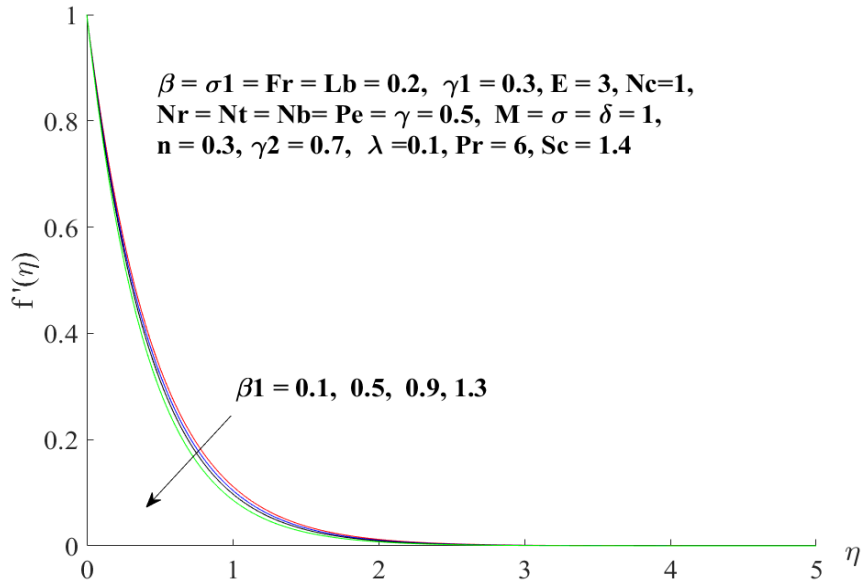

Figure 4.4: Effect of β_1 on $f'(\eta)$

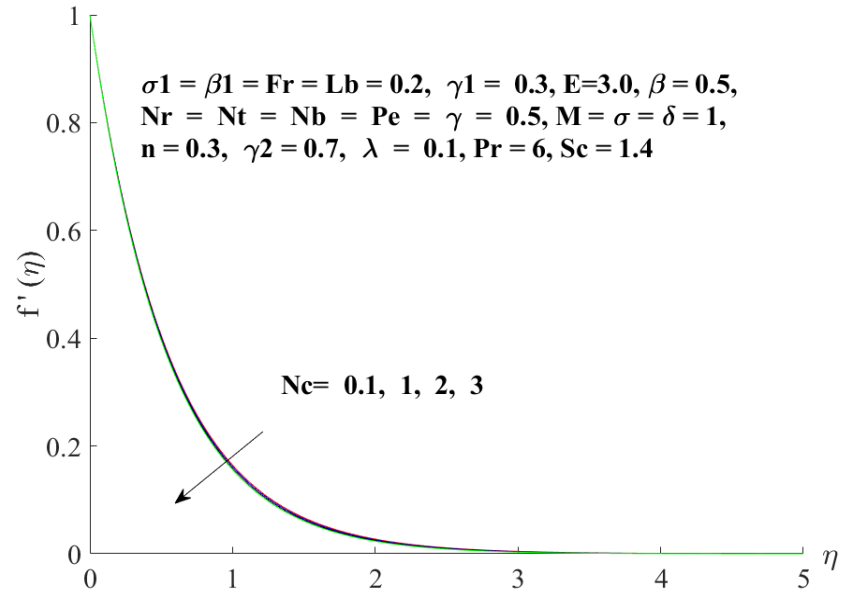

Figure 4.5: Effect of N_c on $f'(\eta)$

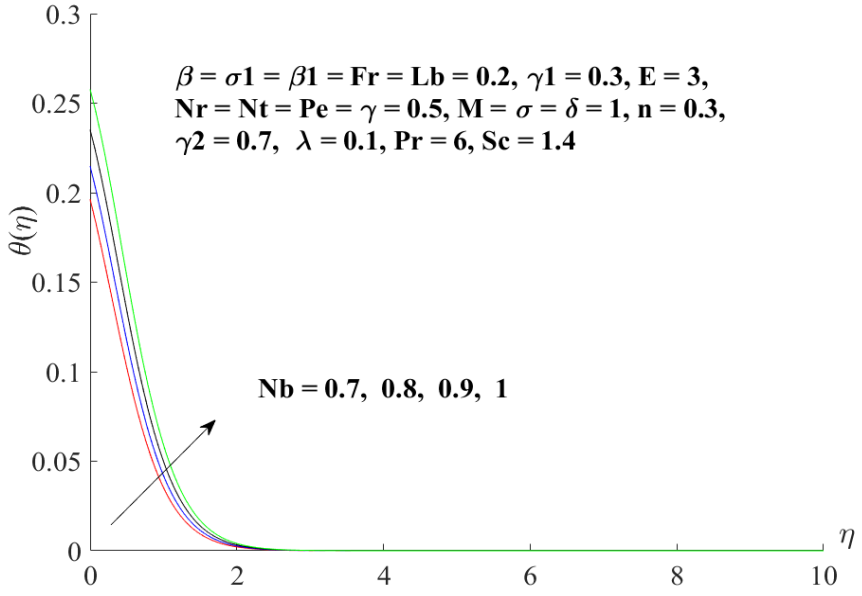

Figure 4.6: Effect of Nb on $\theta(\eta)$

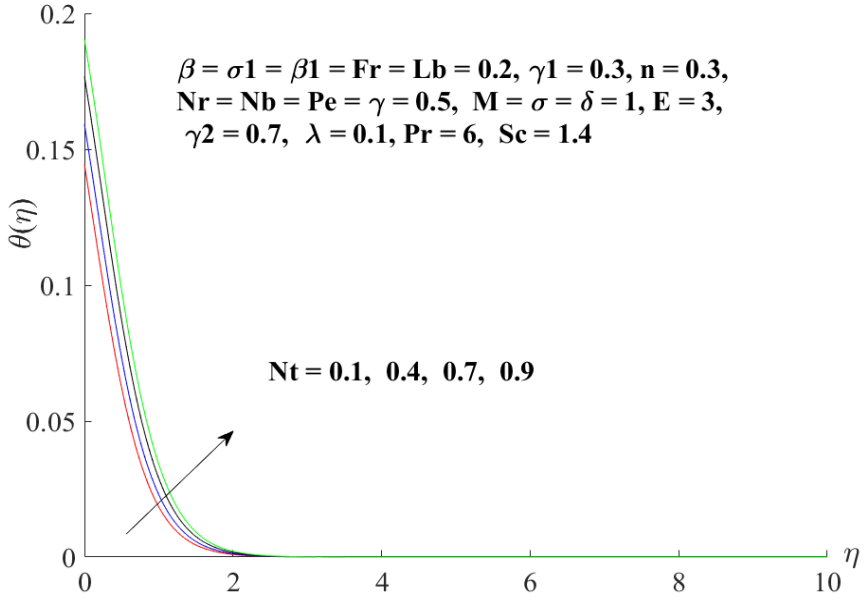

Figure 4.7: Effect of Nt on $\theta(\eta)$

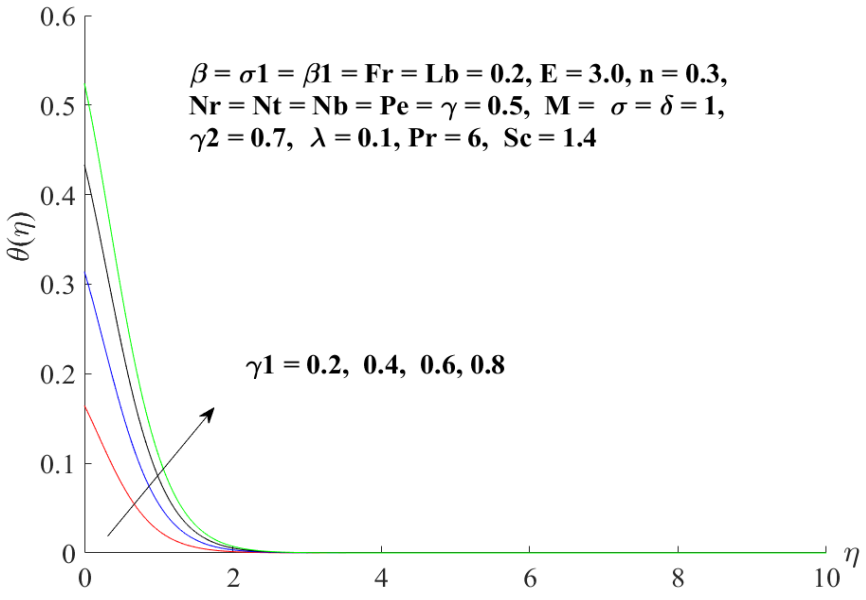

Figure 4.8: Effect of γ_1 on $\theta(\eta)$

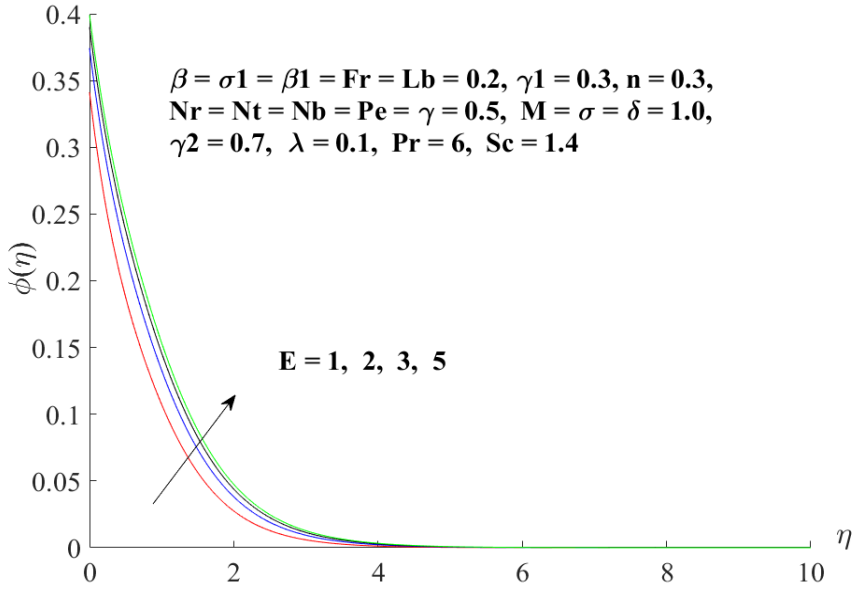

Figure 4.9: Effect of E on $\phi(\eta)$

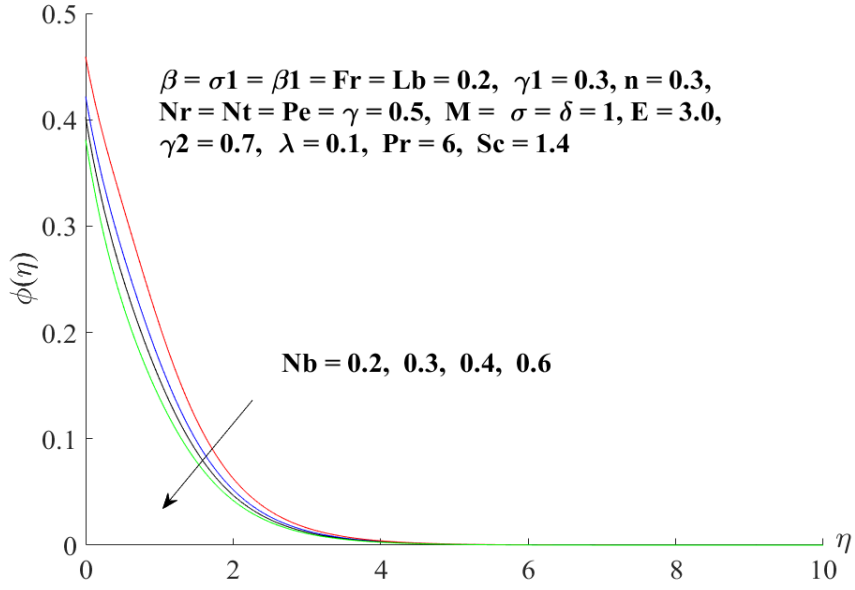

Figure 4.10: Effect of Nb on $\phi(\eta)$

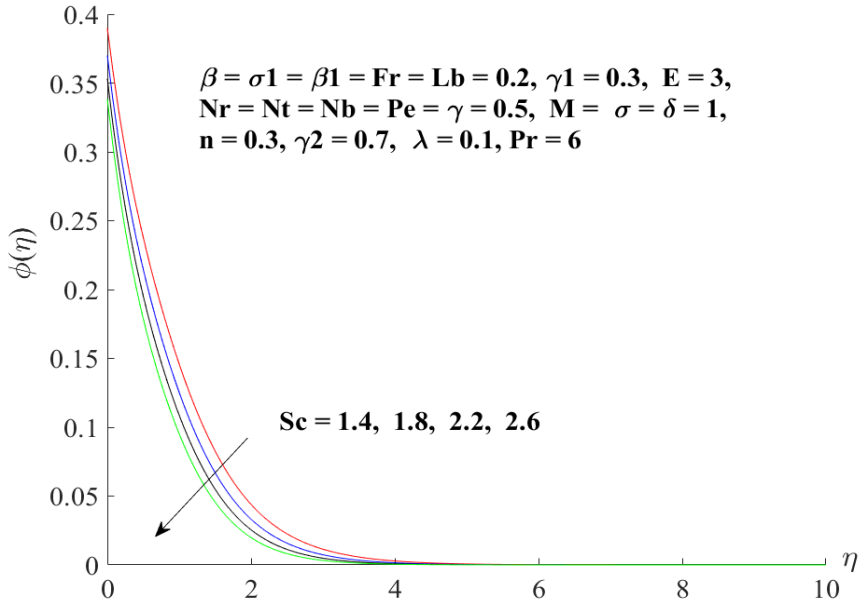

Figure 4.11: Effect of Sc on $\phi(\eta)$

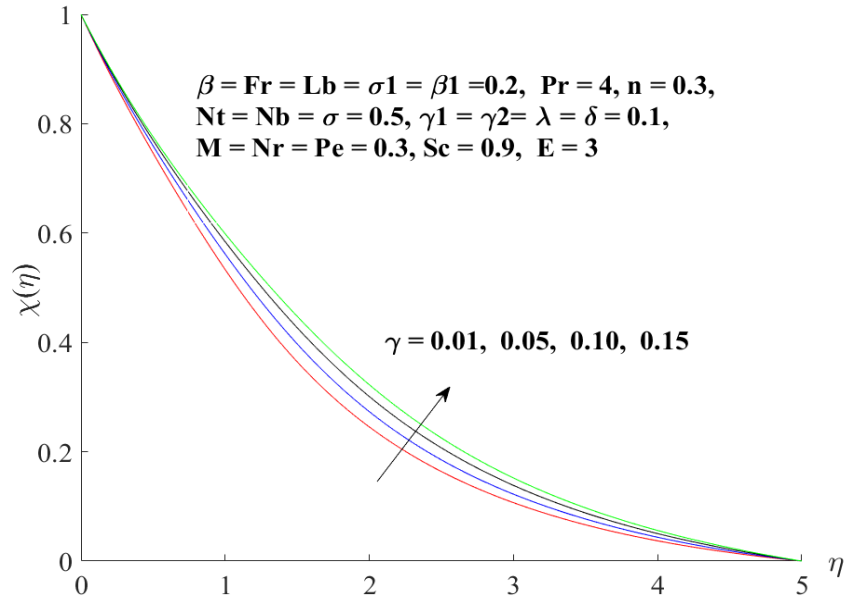

Figure 4.12: Effect of γ on $\chi(\eta)$

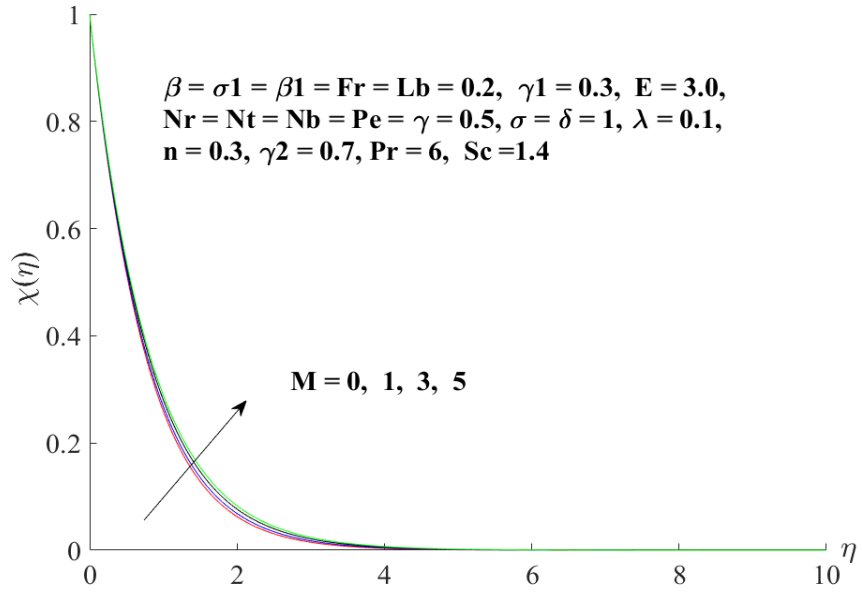

Figure 4.13: Effect of M on $\chi(\eta)$

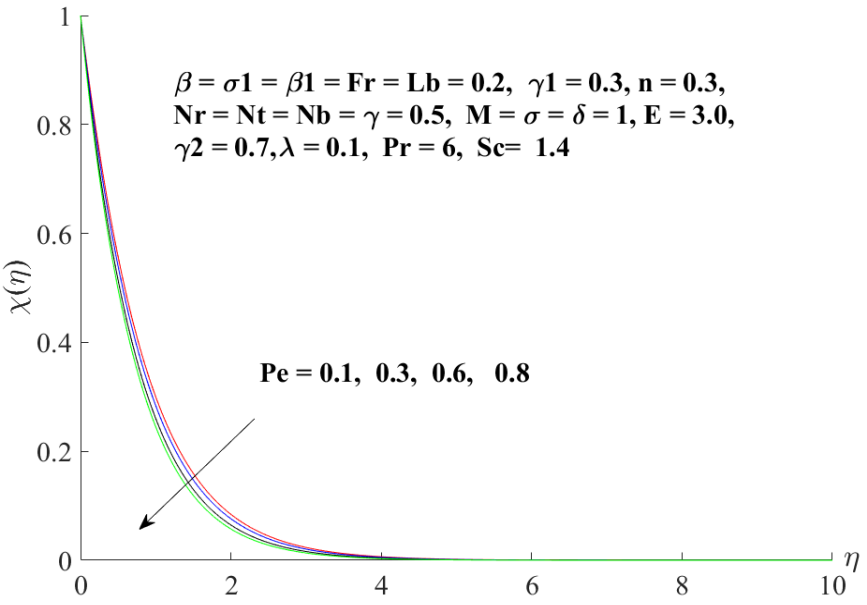

Figure 4.14: Effect of Pe on $\chi(\eta)$

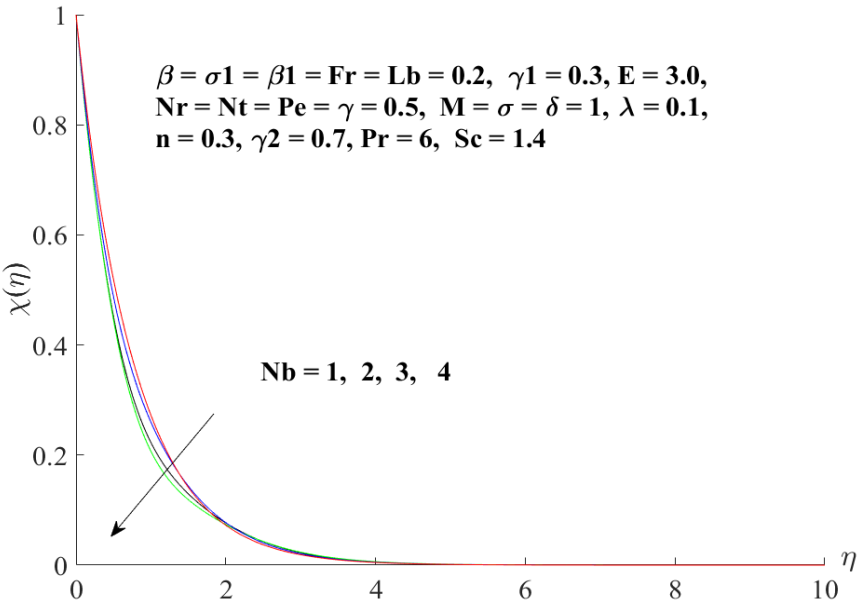

Figure 4.15: Effect of Nb on $\chi(\eta)$

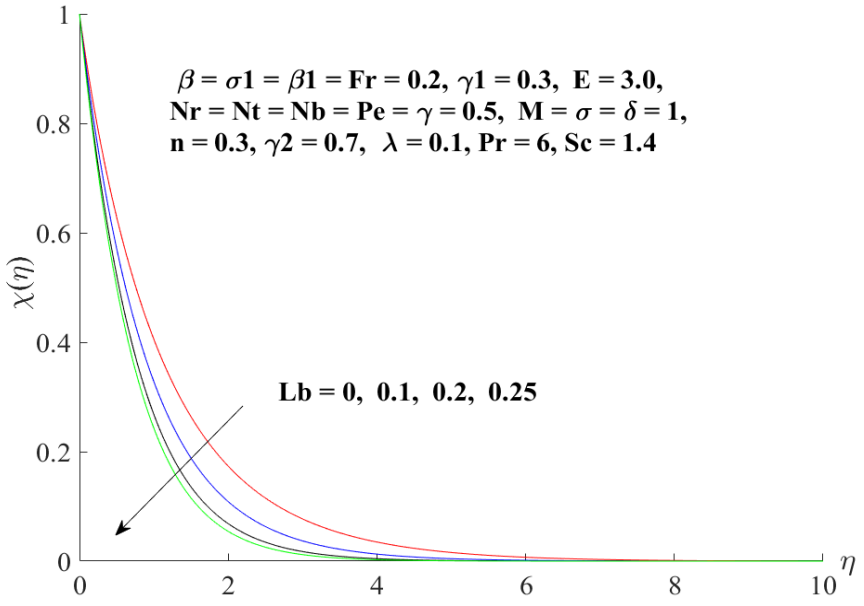

Figure 4.16: Effect of Lb on $\chi(\eta)$

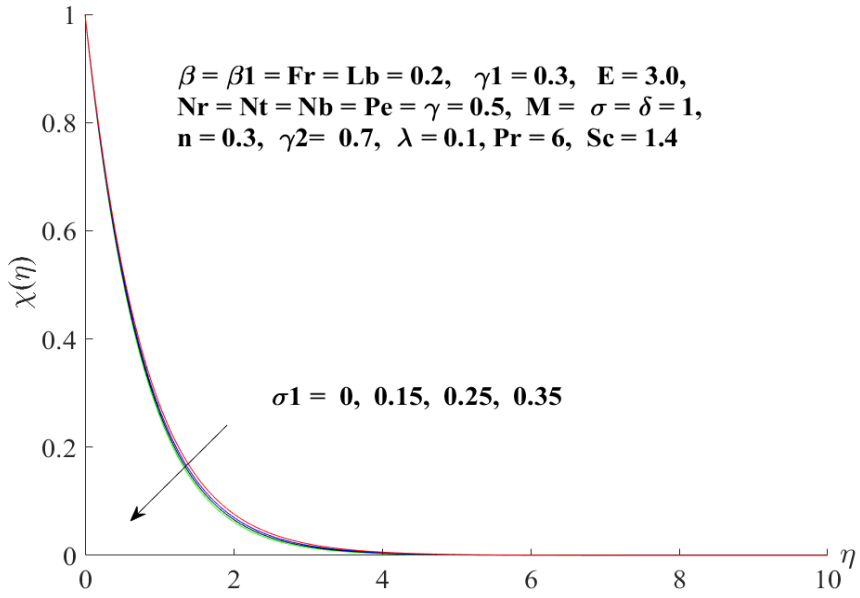

Figure 4.17: Effect of σ_1 on $\chi(\eta)$

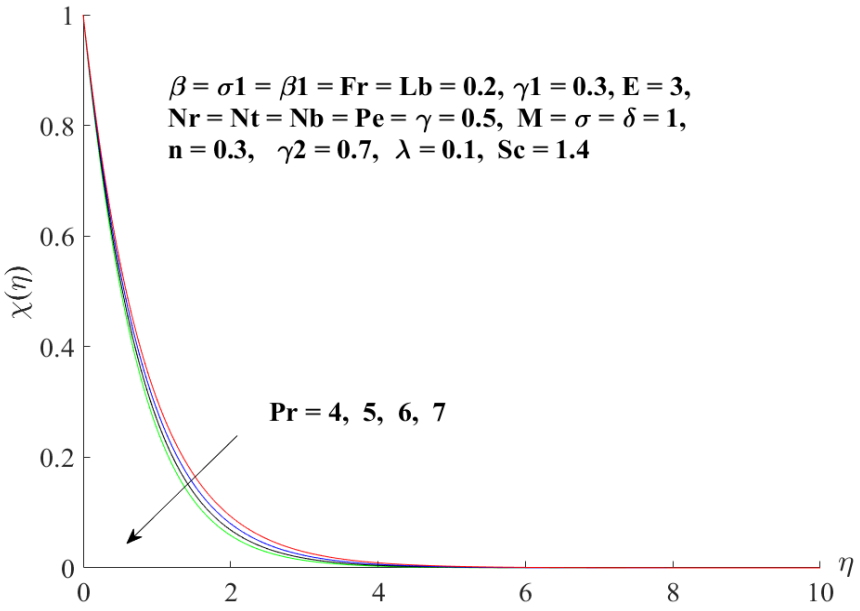

Figure 4.18: Effect of Pr on $\chi(\eta)$

Table 4.1:Numeric values of Nusselt number for different variables.

γ	Nb	Nt	γ_1	γ_2	$Nu_z\,(\mathrm{Re}_z)^{-1/2}$
0.1	0.5	0.5	0.2	0.7	0.167810
0.2					0.168491
0.3					0.169115
0.2	0.1				0.177014
	0.2				0.175197
	0.3				0.173187
	0.5	0.1			0.172091
		0.2			0.171259
		0.3			0.170384
		0.5	0.5		0.319109
			0.7		0.375375
			0.9		0.412207
			0.2	0.5	0.170700
				0.8	0.167494
				1.0	0.165685

Table 4.2: Numeric values of Sherwood number for different variables.

γ	Nb	Nt	γ_2	E	$Sh_z\,(\mathrm{Re}_z)^{-1/2}$
0.1	0.5	0.5	0.7	3	0.368240
0.2					0.389032
0.3					0.407098
0.2	0.1				0.217775
	0.2				0.323627
	0.3				0.359406
	0.5	0.1			0.409086
		0.2			0.403232
		0.3			0.397913
		0.5	0.5		0.311650
			0.8		0.421857
			1.0		0.478531
			0.7	4	0.383759
				5	0.381652
				6	0.380864

Table 4.3: Numeric values of Density number of motile microorganisms for different variables.

γ	σ_1	M	Lb	Pe	Pr	Nb	$Nn_z\left(\mathrm{Re}_z\right)^{-1/2}$
0.1	0.3	1	0.2	0.5	6	0.5	0.99568
0.2							1.09632
0.3							1.19198
0.2	0.3						1.85492
	0.4						1.91332
	0.5						1.97172
	0.3	0					1.83388
		1					1.82178
		2					1.81149
		1	0.2				1.79655
			0.3				1.93032
			0.4				2.04992
			0.2	0.6			1.13367
				0.7			1.16993
				0.8			1.20638
				0.5	6		1.09761
					7		1.15944
					8		1.21782
					6	0.4	1.78211
						0.5	1.79652
						0.6	1.81415

Chapter 5

Conclusions and future work

In this thesis two problems have been analysed where first problem is about review paper and second problem is an extension work. Final remarks of both the problems are as follows:

5.1 Chapter 3

In this section, we have studied the mixed convection Casson nanofluid flow over a strectching barrel along with convective boundary conditions. Problem is examined analytically by making use of renowned Homotopy Analysis method. The significant features of the problem are:

- Fluid flow exhibits an incresing behaviour on escalating values of mixed convection parameter.
- Rise in Casson fluid parameter and the Hartman number redues the fluid flow velocity
- Higher thermophoresis parameter exhibits an enhancement in temperature and concentration distributions.
- Temperature profile rises for larger values of Brownian motion parameter.

- Higher estimates of Biot number boosts in the temperature as well as the concentration.
- The concentration reduces for the escalating values of Brownian motion parameter.
- Heat and mass transfer rate are the decreasing function of high thermophoresis parameter.

5.2 Chapter 4

The present consideration is to analyze the Casson nanofluid flow over a stretchable cylinder with Darcy-Forchheimer spongy structure. Additional effects of Arrhenius Activation energy is also considered. The novelty of the presented model is enhanced by including the influence of motile gyrotactic microorganisms with convective boundary condition. Solution (numerical) of the problem is attained via MATLAB software function bvp4c. The significant observations of the problem are appended as follows:

- The velocity profile is lessening function of Darcy-Forchheimer number.
- The temperature of the fluid expands for escalating estimates of Brownian motion parameter as well as for thermophoresis parameter.
- Incrasing values of activation energy enhances the concentration while reduction is seen in the Sherwood number.
- For increasing estimates of Brownian motion variable, the concentration is on the decline.
- Microorganisms profile dwindles for higher values of Peclet number and Bio-convection Lewis number.
- Microorganisms profile is in direct relation with Hartman number.

- The density of motile microorganisms is dwindled for large values of Bio-convection constant.
- The density number of microorganisms enhances on increasing values of curvature parameter, Prandtl number and Brownian motion parameter while diminishes for Hartman number.

5.3 Future work

In this work, the effects of activation energy and Bio-convection on Casson nanofluid have been analyzed. However, there remains a need to further build on the current work so as to bring improvement about the concerned discourse. Few interesting possible extensions that could be researched in future are as follows:

- Any other non-Newtonian fluid along with appropriate boundary conditions.
- The Tiwari and Das model may be adopted with appropriate combination of nano particles and the base fluid.

Bibliography

[1] Imtiaz, M., Hayat, T., & Alsaedi, A. (2016). Mixed convection flow of Casson nanofluid over a stretching cylinder with convective boundary conditions. Advanced Powder Technology, 27(5), 2245-2256.

[2] Mukhopadhyay, S. (2011). Effects of slip on unsteady mixed convective flow and heat transfer past a porous stretching surface. Nuclear engineering and design, 241(8), 2660-2665.

[3] Hayat, T., Shehzad, S. A., Alsaedi, A., & Alhothuali, M. S. (2012). Mixed convection stagnation point flow of Casson fluid with convective boundary conditions. Chinese Physics Letters, 29(11), 114704.

[4] Turkyilmazoglu, M. (2013). The analytical solution of mixed convection heat transfer and fluid flow of a MHD viscoelastic fluid over a permeable stretching surface. International Journal of Mechanical Sciences, 77, 263-268.

[5] Shehzad, S. A., Alsaedi, A., Hayat, T., & Alhuthali, M. S. (2014). Thermophoresis particle deposition in mixed convection three-dimensional radiative flow of an Oldroyd-B fluid. Journal of the Taiwan Institute of Chemical Engineers, 45(3), 787-794.

[6] Xu, H., & Pop, I. (2014). Mixed convection flow of a nanofluid over a stretching surface with uniform free stream in the presence of both nanoparticles and gyrotactic microorganisms. International Journal of Heat and Mass Transfer, 75, 610-623.

[7] Choi, S. U., & Eastman, J. A. (1995). Enhancing thermal conductivity of fluids with nanoparticles (No. ANL/MSD/CP-84938; CONF-951135-29). Argonne National Lab., IL (United States).

[8] Eastman, J. A., Choi, S. U. S., Li, S., Yu, W., & Thompson, L. J. (2001). Anomalously increased effective thermal conductivities of ethylene glycol-based nanofluids containing copper nanoparticles. Applied physics letters, 78(6), 718-720.

[9] Crane, L. J. (1970). Flow past a stretching plate. Zeitschrift für angewandte Mathematik und Physik ZAMP, 21(4), 645-647.

[10] Malik, M. Y., Naseer, M., Nadeem, S., & Rehman, A. (2014). The boundary layer flow of Casson nanofluid over a vertical exponentially stretching cylinder. Applied Nanoscience, 4(7), 869-873.

[11] Ramesh, G. K., Kumar, K. G., Shehzad, S. A., & Gireesha, B. J. (2018). Enhancement of radiation on hydromagnetic Casson fluid flow towards a stretched cylinder with suspension of liquid-particles. Canadian Journal of Physics, 96(1), 18-24.

[12] Hayat, T., Shah, F., Khan, M. I., & Alsaedi, A. (2017). Framing the performance of heat absorption/generation and thermal radiation in chemically reactive Darcy-Forchheimer flow. Results in Physics, 7, 3390-3395.

[13] Sajid, T., Sagheer, M., Hussain, S., & Bilal, M. (2018). Darcy-Forchheimer flow of Maxwell nanofluid flow with nonlinear thermal radiation and activation energy. AIP Advances, 8(3), 035102.

[14] Muskat, M. (1946). The flow of homogeneous fluids through porous media (No. 532.5 M88).

[15] Rashid, S., Khan, M. I., Hayat, T., Ayub, M., & Alsaedi, A. (2019). Darcy–Forchheimer flow of Maxwell fluid with activation energy and thermal radiation over an exponential surface. Applied Nanoscience, 1-11.

[16] Rashid, M., Hayat, T., & Alsaedi, A. (2019). Entropy generation in Darcy–Forchheimer flow of nanofluid with five nanoarticles due to stretching cylinder. Applied Nanoscience, 9(8), 1649-1659..

[17] Waqas, M., Naz, S., Hayat, T., & Alsaedi, A. (2019). Numerical simulation for activation energy impact in Darcy–Forchheimer nanofluid flow by impermeable cylinder with thermal radiation. Applied Nanoscience, 1-10.

[18] Hayat, T., Aziz, A., Muhammad, T., & Alsaedi, A. (2019). Effects of binary chemical reaction and Arrhenius activation energy in Darcy–Forchheimer three-dimensional flow of nanofluid subject to rotating frame. Journal of Thermal Analysis and Calorimetry, 136(4), 1769-1779.

[19] Saeed, A., Tassaddiq, A., Khan, A., Jawad, M., Deebani, W., Shah, Z., & Islam, S. (2020). Darcy-Forchheimer MHD Hybrid Nanofluid Flow and Heat Transfer Analysis over a Porous Stretching Cylinder. Coatings, 10(4), 391.

[20] Mustafa, M., Khan, J. A., Hayat, T., & Alsaedi, A. (2017). Buoyancy effects on the MHD nanofluid flow past a vertical surface with chemical reaction and activation energy. International Journal of Heat and Mass Transfer, 108, 1340-1346.

[21] Bestman, A. R. (1990). Natural convection boundary layer with suction and mass transfer in a porous medium. International Journal of Energy Research, 14(4), 389-396.

[22] Maleque, K. (2013). Effects of exothermic/endothermic chemical reactions with Arrhenius activation energy on MHD free convection and mass transfer flow in presence of thermal radiation. Journal of Thermodynamics, 2013.

[23] Abbas, Z., Sheikh, M., & Motsa, S. S. (2016). Numerical solution of binary chemical reaction on stagnation point flow of Casson fluid over a stretching/shrinking sheet with thermal radiation. Energy, 95, 12-20.

[24] Lu, D., Ramzan, M., Ullah, N., Chung, J. D., & Farooq, U. (2017). A numerical treatment of radiative nanofluid 3D flow containing gyrotactic microorganism with anisotropic slip, binary chemical reaction and activation energy. Scientific reports, 7(1), 17008.

[25] Huang, C. J. (2019). Arrhenius Activation Energy Effect on Free Convection About a Permeable Horizontal Cylinder in Porous Media. Transport in Porous Media, 128(2), 723-740.

[26] Avramenko, A. A., & Kuznetsov, A. V. (2004). Stability of a suspension of gyrotactic microorganisms in superimposed fluid and porous layers. International communications in heat and mass transfer, 31(8), 1057-1066.

[27] Mehryan, S. A. M., Kashkooli, F. M., Soltani, M., & Raahemifar, K. (2016). Fluid flow and heat transfer analysis of a nanofluid containing motile gyrotactic microorganisms passing a nonlinear stretching vertical sheet in the presence of a non-uniform magnetic field; numerical approach. PloS one, 11(6), e0157598.

[28] Hussain, S. A., Muhammad, S., Ali, G., Shah, S. I. A., Ishaq, M., Shah, Z., ... & Naeem, M. (2018). A bioconvection model for squeezing flow between parallel plates containing gyrotactic microorganisms with impact of thermal radiation and heat generation/absorption. Journal of Advances in Mathematics and Computer Science, 1-22.

[29] Ali Lund, L., Omar, Z., Khan, I., Raza, J., Bakouri, M., & Tlili, I. (2019). Stability Analysis of Darcy-Forchheimer Flow of Casson Type Nanofluid Over an Exponential Sheet: Investigation of Critical Points. Symmetry, 11(3), 412.

[30] Rashad, A. M., & Nabwey, H. A. (2019). Gyrotactic mixed bioconvection flow of a nanofluid past a circular cylinder with convective boundary condition. Journal of the Taiwan Institute of Chemical Engineers, 99, 9-17.

[31] Bhatti, M. M., Mishra, S. R., Abbas, T., & Rashidi, M. M. (2018). A mathematical model of MHD nanofluid flow having gyrotactic microorganisms with thermal radiation and chemical reaction effects. Neural Computing and Applications, 30(4), 1237-1249.

[32] Ramzan, M., Chung, J. D., & Ullah, N. (2017). Radiative magnetohydrodynamic nanofluid flow due to gyrotactic microorganisms with chemical reaction and nonlinear thermal radiation. International Journal of Mechanical Sciences, 130, 31-40.

[33] Alsaedi, A., Khan, M. I., Farooq, M., Gull, N., & Hayat, T. (2017). Magnetohydrodynamic (MHD) stratified bioconvective flow of nanofluid due to gyrotactic microorganisms. Advanced Powder Technology, 28(1), 288-298.

[34] Khan, W. A., Rashad, A. M., Abdou, M. M. M., & Tlili, I. (2019). Natural bioconvection flow of a nanofluid containing gyrotactic microorganisms about a truncated cone. European Journal of Mechanics-B/Fluids, 75, 133-142.

[35] Kuznetsov, A. V. (2005). Thermo-bioconvection in a suspension of oxytactic bacteria. International communications in heat and mass transfer, 32(8), 991-999.

[36] Kuznetsov, A. V. (2005). Investigation of the onset of thermo-bioconvection in a suspension of oxytactic microorganisms in a shallow fluid layer heated from below. Theoretical and Computational Fluid Dynamics, 19(4), 287-299.

[37] Khan, M. N., Khan, W. A., & Tlili, I. (2019). Forced convection of nanofluid flow across horizontal elliptical cylinder with constant heat flux boundary condition. Journal of Nanofluids, 8(2), 386-393.

[38] Makinde, O. D., Iskander, T., Mabood, F., Khan, W. A., & Tshehla, M. S. (2016). MHD Couette-Poiseuille flow of variable viscosity nanofluids in a rotating permeable channel with Hall effects. Journal of Molecular liquids, 221, 778-787.

Saliha MS thesis

ORIGINALITY REPORT

9%	%	%	%
SIMILARITY INDEX	INTERNET SOURCES	PUBLICATIONS	STUDENT PAPERS

PRIMARY SOURCES

1	Submitted to Higher Education Commission Pakistan Student Paper	2%
2	Hina Sadaf, Sara I. Abdelsalam. "Adverse effects of a hybrid nanofluid in a wavy non-uniform annulus with convective boundary conditions", RSC Advances, 2020 Publication	<1%
3	Submitted to National Tsing Hua University Student Paper	<1%
4	Maria Imtiaz, Tasawar Hayat, Ahmed Alsaedi. "Mixed convection flow of Casson nanofluid over a stretching cylinder with convective boundary conditions", Advanced Powder Technology, 2016 Publication	<1%
5	www.nature.com Internet Source	<1%
6	www.mdpi.com Internet Source	<1%

05/10/2020